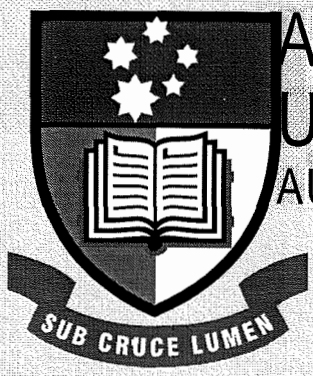

ADELAIDE
UNIVERSITY
AUSTRALIA

Nd isotopic and geochemical constraints on provenance of sedimentary rocks in the Officer Basin, Australia: implications for the duration of the intracratonic Petermann Orogeny

Ben Wade

Supervisors:
Martin Hand
Karin Barovich

12th November 2001

This paper is submitted as partial fulfilment for the Honours degree of Bachelor of Science in Geology

Table of Contents

List of Tables

List of Figures

Abstract

Nd isotopic data from Neoproterozoic to Ordovician sedimentary rocks in the eastern Officer Basin in southern Australia highlight the evolving provenance roles of the Gawler Craton and Musgrave Block basement complexes that bound the Officer Basin.

Initial ε_{Nd} values of around –16 for the early Neoproterozoic basal sequences (Pindyin Sandstone, Alinya Formation, and Tarlina Sandstone) indicate they were largely derived from the Archaean to Palaeoproterozoic Gawler Craton, which bounds the Officer Basin to the south. At around 640 Ma a major excursion of initial ε_{Nd} values in the sedimentary sequence to around –9 indicates significant unroofing of the Mesoproterozoic Musgrave Block, which forms the northern margin of the basin. The uplift of the Musgrave Block at around 640 Ma is interpreted to mark the onset of the intracratonic Petermann Orogeny, which was a major orogenic event that shaped the lithospheric architecture of southern central Australia. Combined with existing isotopic and stratigraphic data, the isotope data from the eastern Officer Basin suggest that the Petermann Orogeny was a relatively long-lived event or series of events spanning a duration greater than 100 Ma.

The change in intial ε_{Nd} is accompanied by geochemical data that indicates slight elevation of mafic trace element indicators in the mid to late Neoproterozoic (Murnaroo Formation and Dey Dey Mudstone, Mena Mudstone Member), and earliest Cambrian (Arcoeillinna Sandstone). This is interpreted as contribution to the basin from the Musgrave Block, which is as a whole more mafic than the Gawler Craton.

Subsequent to 640 Ma, ε_{Nd} values of syn-Petermann Orogeny sediments diverge from the Musgrave Block trend, suggesting that there was an ongoing contribution from the Gawler Craton, despite the deposition of the sequences in the geographic foreland of the Petermann Orogen. The return toward a Gawler Craton provenance suggests that to a large extent, sediment derived from the Petermann Orogen bypassed the eastern Officer Basin for much of the Petermann Orogeny.

Keywords: Australia; Petermann Orogeny; Provenance; Sm-Nd isotopes

1. Introduction

The Neoproterozoic to mid-Palaeozoic intracratonic Officer Basin in southern Australia is one of a number of basins that together formerly comprised the Centralian Superbasin (Fig. 1, Walter et al., 1995). The Centralian Superbasin was subsequently dissected into a southern fragment (Officer Basin), and a northern fragment (incorporating the Amadeus, Georgina, Ngalia, Officer and Savory Basins) during the Petermann Orogeny (Hoskins and Lemon, 1995; Moussavi-Harami and Gravestock, 1995; Walter et al., 1995; Lindsay and Leven, 1996). The exhumed Musgrave Block forms the northern margin of the Officer Basin. On its southern margin, the Officer Basin is bordered by the Archaean-Palaeoproterozoic Gawler Craton (Fig. 1). In general, sediment thickness in the eastern Officer Basin increases northwards towards the Musgrave Block. In the eastern Officer Basin the entire sedimentary package reaches a thickness of 10km in the Munyarai Trough (Fig. 1). The successions within the eastern Officer Basin are composed of Neoproterozoic-Tertiary shales, mudstones, siltstones, sandstones, limestones, and minor volcanics (Fig. 2). Although the Officer Basin is Australia's largest intracratonic basin, as yet there are no data constraining the provenance of sedimentary rocks within it.

This paper presents Nd isotope and geochemical data from the Early Neoproterozoic to Ordovician sedimentary interval of the eastern Officer Basin. The application of geochemical sedimentary provenance can be effectively utilised to tackle geological problems such as discriminating sedimentary sources (e.g. Slack and Stevens, 1994; Dabard et al., 1996; Garzione et al., 1997), and constraining the timing and duration of tectonic events (e.g. Turner et al., 1993; Boghossian et al., 1996; Li et al., 1996). The assumptions made when using rare earth elements (REE) as provenance indicators are that they are not modified by metamorphism and diagenesis, and that the REE's are quantitatively transported in the detrital component and not fractionated by sedimentary processes such as heavy mineral sorting (e.g. McLennan and Taylor, 1982; Crichton and Condie, 1993; Ugidos et al., 1997).

There are two aims to this study:

The primary aim is to utilise the provenance of successions within the eastern Officer Basin as a tool to place temporal constraints on the intracratonic Petermann Orogeny, which to a large extent has shaped the morphology of the Officer Basin (e.g. Hoskins and Lemon, 1995; Moussavi-Harami and Gravestock, 1995). Geochemical and Nd isotopic analyses of sedimentary rocks within the Officer Basin should determine the time at which the erosion of

the Musgrave Block began to dominate the basin input, signifying initiation of unroofing of the Musgrave Block during the Petermann Orogeny.

There are two general models for the timing and duration of the Petermann Orogeny. One model suggests that the Petermann Orogeny began at around 650 Ma and continued to approximately 530 Ma (Shaw, 1991; Calver and Lindsay, 1998). The second model suggests that the Petermann Orogeny was a relatively short lived event, spanning *ca.* 580-540 Ma (e.g. Hoskins and Lemon, 1995; Lindsay and Leven, 1996; Camacho and McDougall, 2000). Discriminating between these two models has important implications for the mechanisms that lead to the development of the Petermann Orogeny, and more generally, the mechanisms that lead to intracratonic deformation.

The second aim of this study is to initiate a database on the source of sequences in the Officer Basin, in order to begin to build up provenance models for the Centralian Superbasin in its entirety.

2. Geological Setting

The Officer Basin in southern central Australia is a large ensialic basin (*ca*. 300 000 km^2), which initially formed during the Neoproterozoic *ca*. 820 m.y. ago (e.g. Moussavi-Harami and Gravestock, 1995; Lindsay and Leven, 1996). The Officer Basin was initially part of a larger depositional system termed the Centralian Superbasin, occupying ~2 million km^2 of central Australia (Preiss and Forbes, 1981; Walter et al., 1995; Preiss, 2000; Fig. 1). Through two fragmentation events (the Petermann Orogeny and the mid-Palaeozoic Alice Springs Orogeny), the Centralian Superbasin was subsequently divided into the series of presently preserved basins (e.g. Amadeus, Georgina, Ngalia, Savory and Officer Basins; Fig. 1).

The morphological evolution of the eastern Officer Basin can be described in four phases (e.g. Hoskins and Lemon, 1995; Moussavi-Harami and Gravestock, 1995).

Stage 1 involves initiation of the Centralian Superbasin, a giant sag basin linked to NE-SW crustal extension *ca*. 820 Ma (e.g. Moussavi-Harami and Gravestock, 1995; Walter et al., 1995), and deposition of the Pindyin Sandstone and Alinya Formation (Fig. 2).

Stage 2 comprises deposition of the mid-late Neoproterozoic Lake Maurice and Ungoolya Groups, which predate and span the initial stages of the Petermann Orogeny. The timing of north-south compression during the latter part of this stage is largely unclear, and could be as early as *ca*. 650 Ma (Shaw, 1991; Calver and Lindsay, 1998), or as late as *ca*. 580 Ma (e.g. Hoskins and Lemon, 1995; Lindsay and Leven, 1996; Camacho and McDougall, 2000). The uplift of the Musgrave Block severed the connection between the Officer Basin and the Centralian Superbasin.

Stage 3 is marked by the onset of deposition of early-mid Cambrian Marla Group sediments. Sediments characterising stage 3 are interpreted to have been deposited within a mildy extensional regime (Lindsay and Leven, 1996). Cambrian deposition in the eastern Officer Basin was halted by the mid-late Cambrian Delamerian Orogeny which inverted the Adelaide Rift Complex to the east of the Officer Basin (Fig. 1), and resulted in uplift and erosion of Cambrian sediments in the Officer Basin (Hoskins and Lemon, 1995).

Stage 4 is defined by deposition of Munda Group sediments during inferred early Ordovician N-S extension (Hoskins and Lemon, 1995; Moussavi-Harami and Gravestock, 1995). Deposition of the Munda Group was followed by the Alice Springs Orogeny @ *ca.* 360 Ma which resulted in the further uplift of the Musgrave Block (e.g. Korsch and Lindsay,

1989; Shaw and Black, 1991; Shaw et al., 1991; Hand and Sandiford, 1999), resulting in the deposition of a thick wedge of syn-orogenic Devonian sediments in the northeastern Officer Basin.

The stratigraphy of the Officer Basin is poorly known compared to other fragments of the Centralian Superbasin such as the Amadeus Basin (e.g. Lindsay, 1987; Hoskins and Lemon, 1995; Walter et al., 1995; Lindsay and Leven, 1996). Outcrop in the basin is poor and displays only limited sections of the entire stratigraphy of the basin due to generally shallow dips of the strata. In addition there are relatively few stratigraphic wells.

Figure 2 shows the currently accepted stratigraphic framework for the basin (Benbow, 1982; Gatehouse et al., 1986; Brewer et al., 1987; Stainton et al., 1988; Zang, 1994, 1995). Recently, correlation of Neoproterozoic sequences has been vastly improved through analysis of acritarch assemblages, which can be utilised as a reliable tool in stratigraphic correlation throughout the basin (Zang, 1994, 1995). Sequence stratigraphy has also been used as an aid to correlation (Sukanta, 1993; Moussavi-Harami and Gravestock, 1995). Interbasinal correlations across the entirety of the Centralian Superbasin have been proposed by various authors in an effort to determine the depositional setting of sediments and to constrain the age of sedimentation (e.g. Preiss and Forbes, 1981; Plumb, 1985; Walter et al., 1995). These interbasinal correlations show that although some correlative successions have similar characteristics, there appears to be correlative gaps for some successions (Preiss and Forbes, 1981; Walter et al., 1995), and demonstrates the uncertainty of correlations of units across basins. By establishing provenance data for successions in different parts of the Centralian Superbasin, stratigraphic correlation can be improved, resulting in a more coherent framework for the development of the Centralian Superbasin.

3. **Sampling Methods**

Figure 1 shows the location of drill holes sampled for this study, and Figure 2 shows the generalised stratigraphic column for the basin with the sampled units indicated. The sample lithologies and drillholes are presented in Table 1. The units sampled were chosen to obtain a relative spread of data from the Neoproterozoic through to the Late Ordovician, thus essentially spanning most of the depositional time of the eastern Officer Basin. Sampling was concentrated around units of apparent Petermann Orogeny age (i.e., Mena Mudstone Member, Relief Sandstone; e.g Hoskins and Lemon, 1995; Moussavi-Harami and Gravestock, 1995) and to either side of these sequences in the initial expectation that this is the stage in the basin evolution where the major change in provenance signal would occur (Fig. 2).

The sampling method was also constructed to observe changes in sedimentary provenance of the same unit in different parts of the basin. Units of Pre-Petermann Orogeny age sampled in duplicate include the Murnaroo Formation sampled from Lake Maurice 1 located proximal to the Gawler Craton, and from Munta 1 located closer to the Musgrave Block; and the Dey Dey Mudstone from drill holes Murnaroo 1 and Karlaya 1 (Fig 1). Those units of apparent Petermann Orogeny age include the Relief Sandstone from Meramangye 1 and Observatory Hill 1, and the Observatory Hill Formation from Marla 3 and Observatory Hill 1 (Fig 2).

The sampled lithologies are primarily mudstones and sandstones, with minor shales and siltstones. The isotopic composition of mudstones is particularly important as they record an average of the source regions rather than a point source (e.g. Anderson and Samson, 1995). As the REEs are generally reasonably resistant to fractionation during processes such as weathering and diagenesis (e.g. McCulloch and Wasserburg, 1978; McLennan and Taylor, 1982; McLennan et al., 1993), the Nd isotopic ratios of clastic sedimentary rocks calculated at their time of deposition appear to be robust (e.g. McLennan et al., 1989). To avoid the potential problems associated with fractionation of REE during sediment transport, the interpretations in this paper are based on initial ε_{Nd} values rather than model ages. Thirty samples were analysed for major and trace elements and twenty samples were analysed for Nd isotopes.

Correlations between units of the Officer Basin, Amadeus Basin, and Adelaide Geosyncline have been summarised by Preiss and Forbes (1981) and Walter et al. (1995). Initial εNd values for the samples have been calculated and are compared to equivalent units in the Amadeus Basin from Zhao et al. (1992), Barovich and Foden (2000), and unpublished

data by Barovich, in order to assess similarities in εNd values for correlative units across the Centralian Superbasin.

4. Analytical Procedures

Samples were cut from quarter core and then cleaned in an ultrasonic bath in order to remove potential interstratigraphic contamination from drilling mud. 15 cms of the clean core which represented the most homogeneous portion of the core was then crushed. Major and trace element data were acquired through the analysis of fused glass disks and pressed pellets respectively, using a Philips PW 1480 X-ray Fluorescence Spectrometer at Adelaide University.

Samples analysed for Sm-Nd isotopic composition were evaporated in HF/HNO_3 overnight, digested in hot HF/HNO_3 in sealed Teflon vials for 5 days, then evaporated to dryness in HF/HNO_3. Samples were evaporated in 6M HCl then sealed with 6M HCl and left on heat overnight. Nd and Sm concentrations were calculated by isotope dilution, with Nd isotope ratios measured by thermal ionisation mass spectrometry on a Finnigan MAT 262 mass spectrometer, and Sm isotope ratios measured on a Finnigan MAT 261 mass spectrometer. Nd blanks range from 79 to 85 pg. The $^{143}Nd/^{144}Nd$ ratio is normalised to $^{146}Nd/^{144}Nd = 0.721903$. The $^{143}Nd/^{144}Nd$ ratio of the La Jolla standard at the Adelaide University laboratory is 0.511810 ± 7 (n=13).

5. Results

Major elements

Major element data for whole rock samples are presented in Table 2 and Figure 3. The SiO_2 range for samples from the eastern Officer Basin are comparable to samples from the Amadeus Basin and Adelaide Geosyncline (55 to 99% versus 48 to 93% versus 49 to 88% respectively, (Turner et al., 1993; Barovich and Foden, 2000)). However, the samples from the eastern Officer Basin differ slightly in that they in part comprise extremely clean sandstones (up to ~100% SiO_2 in the Mt Chandler Sst), similar to the higher end of the range for both the Amadeus Basin and Adelaide Geosyncline suites. Al_2O_3 abundances span a much larger range than both the Amadeus Basin and Adelaide Geosyncline suites (0.15 to 17% versus 10 to 19% versus 3 to 14% respectively, (Turner et al., 1993; Barovich and Foden 2000)).

With increasing SiO_2 content, there is a decrease in TiO_2, Nd, and Zr (Fig 3). There are positive correlations between Al_2O_3, K_2O and TiO_2 for (Fig 3). In addition, there are positive correlations between K_2O and TiO_2 vs SiO_2, and TiO_2 vs Fe_2O_3.

Trace elements

Trace element data for whole rock samples is presented in Table 2 and Figures 4 and 5. There is positive correlation between La and Nd versus Al_2O_3 and La and Nd vs P_2O_5 (Fig 4). Figure 5 shows a positive correlation of Ni and Cr with Al_2O_3. There is no apparent correlation between La/Y and Th/U vs SiO_2, and no apparent correlation between zircon abundance (assumed by Zr ppm) and Zr/Y in shales or sandstones (Fig. 5).

The majority of samples contain Ni, Cr, Sc, and V concentrations less than the Post-Archaean Australian Shale composite (PAAS, Taylor and McLennan, 1985). However, elevated concentrations of Ni, Cr, Sc, and V relative to PAAS occur in samples 2012-990 from the Murnaroo Formation, the single sample from the Arcoeillinna Sandstone, and sample 2012-910 from the Dey Dey Mudstone.

Neodymium isotopes

Sm-Nd isotope data are presented in Table 3, and plotted as ε_{Nd} versus time (Figs. 6a and 6b). Average basement compositions for both the Gawler Craton and Musgrave Block are also shown in Figures 6a and 6b. All but one of the $^{147}Sm/^{144}Nd$ ratios for the Officer Basin suite fall in the range 0.10-0.13. The range of ε_{Nd} (0) values are from –13.8 to –28.4 with the majority falling between –15.7 to –18.9. Initial ε_{Nd} (t) values range from –9.7 to –13.6.

Up to *ca.* 640 Ma, the initial ε_{Nd} values of the samples from the Pindyin Sandstone, Alinya Formation, and Tarlina Sandstone plot relatively close to the Gawler Craton evolution line. At *ca.* 640 Ma there is a large excursion in initial ε_{Nd} towards less negative values. From this point onwards, the trend of sedimentary rock compositions diverges from the Musgrave evolution trend. The large jump in intial ε_{Nd} values at *ca.* 640 Ma, from an initial ε_{Nd} value of –20.7 for the Tarlina Sandstone (sample no. 2012-001; stratigraphic age *ca.* 645 Ma (Zang, 1994, 1995)), to an initial ε_{Nd} value of –9.7 for the Meramangye Formation (sample no. 2012-997; stratigraphic age *ca.* 635 Ma (Zang, 1994, 1995)), occurs over a relatively constricted time interval. The initial ε_{Nd} values of the samples from the *ca.* 620 Ma Murnaroo Formation (sample no. 2012-990 and 2012-015) plot close to the Musgrave Block evolution trajectory.

Data from sedimentary rocks in the Amadeus Basin (Zhao et al., 1992; Barovich and Foden, 2000) are shown in Figure 6b with results from this study. Interbasinal correlations from previous studies (Preiss and Forbes, 1981; Walter et al., 1995) allow comparison of ε_{Nd} values of correlatable units between basins. Of those units which can be compared, ε_{Nd} values from Zhao et al. (1992) are less negative than ε_{Nd} values of comparable units from this study, taking into account that sediments from the Amadeus Basin are derived from a mixture of different sources than the Officer Basin (e.g., Zhao et al., 1992).

Figure 7 shows mafic trace element indicators compared with initial ε_{Nd} values of the eastern Officer Basin rocks. These trace element indicators can be utilised to determine the input of mafic material into a basin (e.g McLennan et al., 1993; Barovich and Foden, 2000). There is a rough trend of increasing ε_{Nd} values with increasing Ni, Cr, Sc, and V.

6. Provenance

Source Characterisation

In comparison with continental margin settings, the source regions for intracratonic basinal sediments are commonly still in place, allowing reasonably detailed source characterisation. Basement to the eastern Officer Basin consists of the Archaean to Palaeoproterozoic Gawler Craton to the south, and the Mesoproterozoic Musgrave Block to the north (Fig. 1). Palaeoproterozoic rocks in the northwestern Gawler Craton consist of upper amphibolite to granulite facies, felsic-mafic gneisses, and granites such as the 1585 Ma Hiltaba Suite (Parker and Lemon, 1982; Rankin et al., 1989; Daly et al., 1998). The Musgrave Block consists of granulite facies felsic gneisses, granites, felsic and mafic granulites, and voluminous mafic-ultramafic intrusives (Major and Conor, 1993; Glikson et al., 1996; Young et al., 1998). The two source regions are quite different in their composition and age, with the Musgrave Block as a whole containing significantly more mafic material than the Gawler Craton (Parker and Lemon, 1982; Glikson et al., 1995; Major and Conor, 1993; Lindsay and Leven, 1996). The two sources are also quite different in their average Nd isotopic characteristics (Musgrave Block (average of 20 data points): $^{147}Sm/^{144}Nd$ = 0.1181 $^{143}Nd/^{144}Nd$ = 0.511896; Gawler Craton (average of 40 data points): $^{147}Sm/^{144}Nd$ = 0.1106 $^{143}Nd/^{144}Nd$ = 0.511354; Zhao et al., 1992; Turner et al., 1993; Creaser, 1995; Schaefer, 1998; Neumann, 2001, Appendix 1).

Major and trace element chemistry

The strong positive correlation of K_2O and TiO_2 with Al_2O_3 in the eastern Officer Basin sedimentary rocks (Fig. 3), suggests control of these elements by minerals such as detrital clays and micas (e.g. Crichton and Condie, 1993). In addition, it is also important to note that a positive correlation between TiO_2 and Fe_2O_3, which implies the presence of Fe-bearing minerals such as ilmenite.

There are two possible explanations for the positive correlations between these major element oxides. Firstly the positive correlations could imply a relatively homogeneous source. Moderate to poor correlations would imply a less mature, and possibly multicomponent source terrane (e.g. Uguidos et al., 1997; Barovich and Foden, 2000). The second possible explanation is that these correlations are controlled by a relatively restricted range of detrital minerals, which have limited compositional ranges. The possibility that the major element data is indicative of a single source terrane appears to contradict the Nd isotope

data that strongly implies input from both the Musgrave Block and the Gawler Craton. Thus, the second explanation of compositional restrictions by detrital minerals is favoured.

It is important to determine the controls on the REE concentrations in sediments, as the REEs are important source indicators (e.g. Garzione et al., 1997; Ugidos et al., 1997). For Nd isotopes to be used confidently in sedimentary provenance studies, it needs to be assessed whether the Sm-Nd isotope systematics have been altered through sedimentary processes such as heavy mineral sorting. It also is important to determine whether coarse-grained lithologies give comparable geochemical results to those of finer grained lithologies such as mudstones. Trace element data for whole rock samples is presented in Table 2 and Figures 4-5. A possible cause of REE fractionation is heavy mineral sorting that leads to zircon fractionation. Zircon has been shown to carry a significant proportion of the REE budget in coarse sandstones (McLennan et al., 1993; Ugidos et al., 1997). By demonstrating that the REEs are not contained in zircon but in the micaceous minerals or clay phases, it can be assumed that heavy mineral fractionation has not occurred, and thus one can confidently use REE's as provenance indicators (McLennan et al., 1990; McLennan et al., 1993; Ugidos et al., 1997).

Figure 5 shows the lack of major variation in Zr/Y with Zr content for both shales and sandstones. The absence of correlation suggests that zircon within the rock controls a minor proportion, if any, of the REE budget (e.g. Crichton and Condie, 1993; Ugidos et al., 1997). This lack of correlation coupled with the positive correlation between La and Nd vs Al_2O_3, and La and Nd vs P_2O_5 shown in Figure 4, suggests that clays and to some extent phosphate minerals control the REE budget (e.g. McLennan, 1989; Caggianelli et al., 1992; Ugidos et al., 1997). The negative correlations of TiO_2, Nd, and Zr with SiO_2 shown in Figure 3 imply that it is quartz dilution that affects the relative abundance of phyllosilicates in the sedimentary rocks and their REE concentrations (e.g. Garzione et al., 1997; Ugidos et al., 1997). The data argue for control of the REE by detrital phases such as clays or micas rather than heavy mineral phases, and thus both the sandstone and mudstone samples give reliable geochemical data.

For the trace element vs silica plots such as La/Y vs SiO_2 (Fig. 5), a relatively constant La/Y ratio is maintained for a large range of SiO_2 concentrations. This suggests that for both coarse and fine grained lithologies (i.e., clean sandstones and shales) as indicated by the range of SiO_2, the relative ratios of important trace element provenance indicators remain relatively constant. This in turn implies that REE, and more importantly for this study, Nd isotopes from

coarse-grained samples within the eastern Officer Basin can be used with confidence in conjunction with fine-grained lithologies.

Trace element data can be used as evidence of input of mafic material into a basin. In particular the compatible elements Sc, Cr, Ni, and V are most commonly used as indicators of a mafic crustal component supplying sediment (e.g. Prame and Pohl, 1994; Li and McCulloch, 1996; Barovich and Foden, 2000). The concentration of trace elements ,is however, affected by the quartz content of the rock, with lower concentrations of trace elements related to increasing quartz content (e.g. Crichton and Condie, 1993; Ugidos et al., 1997). Thus it must be determined if the low concentrations of elements such as Ni and Cr in coarser-grained samples used in this study is due to the high quartz content, or to the lack of mafic contribution to the sample's composition.

Some of the sandstones analysed in this study are extremely quartz rich (e.g. sample 2012-008 from the Pindyin Sandstone and sample 2012-612 from the Mt Chandler Sandstone), and thus the low Ni and Cr concentrations in the sandstones are probably related to the quartz dilution effect reducing the abundance of phyllosilicates, and indirectly the Ni and Cr concentrations, given their covariations with Al_2O_3 (Fig 5). However, as the abundance of Ni and Cr is below PAAS in almost all of the fine-grained samples, the Ni and Cr abundances in the sandstones are interpreted to fall below PAAS also. The slightly elevated concentrations of Ni and Cr in sample 2012-990 from the Murnaroo Formation, the sample from the Arcoeillinna Sandstone, and 2012-910 from the Dey Dey Mudstone, suggest that a minor proportion of mafic crust has contributed to the basin fill.

Neodymium Isotopes

Nd isotopic data from the eastern Officer Basin indicate relatively minor contribution to the basin fill from the Musgrave Block before *ca.* 640 Ma (Fig 6a). The prominent excursion at *ca.* 640 Ma towards a Musgrave-type isotopic composition suggests a large influx of Musgrave Block derived sediments into the basin. From *ca.* 620 Ma, the ε_{Nd} values slowly diverge from the Musgrave evolution line, implying mixing of the Musgrave Block and Gawler Craton.

Erosion of a juvenile mafic source region such as the 800 Ma Neoproterozoic flood basalt province thought to have been present in southern Australia (e.g. Wingate et al., 1998;

Barovich and Foden, 2000), could cause a large influx of less radiogenic mafic material into the depositional system, dramatically affecting the ε_{Nd} values of sediments within the Officer

Basin. Thus it needs to determined if the large excursion in ε_{Nd} values around *ca.* 640 Ma is due to exhumation of the Musgrave Block, or due to input of juvenile mafic material into the basin fill. The samples that plot close to the Musgrave Block ε_{Nd} evolutionary trajectory immediately after the sharp increase in ε_{Nd} values include a sample from the Meramangye Formation (sample 2012-997; stratigraphic age *ca.* 635Ma), and two samples from the Murnaroo Formation (samples 2012-990, and 2012-015; stratigraphic age *ca.* 620 Ma). These contain slightly elevated concentrations of Ni, Cr, Sc, and V concentrations relative to PAAS. The rough correlative trend of increasing ε_{Nd} values with increasing Ni, Cr, Sc, and V (Fig. 7) can be interpreted as minor contribution from a mafic source. Hence it is also possible that the excursion in ε_{Nd} values seen at *ca* 640 Ma is due to the contribution of a juvenile mafic source. However, the hypothesis that this excursion is due to onset of exhumation of the Musgrave Block rather than erosion of a juvenile mafic terrain is favoured for the following reasons.

(1) The rise in initial ε_{Nd} is far too great to be generated by simple incorporation of mafic material into the basin. The increase in ε_{Nd} values at *ca.* 640 Ma display a rise of nearly 11 ε_{Nd} units.

(2) Previous studies have argued for the existence of a large Neoproterozoic flood basalt province in southern Australia related to the breakup of the supercontinent Rodinia (e.g. Wingate et al., 1998; Barovich and Foden, 2000). The emplacement of this flood basalt is thought to have occurred around 800 Ma (Wingate et al., 1998). However the rise seen in the ε_{Nd} values from the current study occurs approximately 160 million years after the emplacement of the flood basalt.

(3) The accompanying large increase in concentration of elements such as Ni, Cr, Sc, and V that would be expected to accompany the erosion of a large mafic terrain is not present. Thus it is more reasonable that this excursion at *ca* 640 Ma is due to onset of erosion of the Musgrave Block, and the slight rise above PAAS in mafic element indicators is due to erosion of mafic bodies within the Musgrave Block such as the 1200 Ma Giles Complex (e.g. Glikson et al., 1995).

Initial ε_{Nd} values for sedimentary rocks from the Amadeus Basin have been plotted on Figure 6b. Comparable units from the current study include the Pindyin Sandstone (correlatable with the Heavitree Quartzite), Alinya Formation (correlatable with Bitter

Springs Formation), Murnaroo Formation (correlatable with the Pioneer Sandstone) and the Dey Dey Mudstone (correlatable with the Pertatataka Formation). For each one of these

sedimentary unit pairs, ε_{Nd} values for sediments from the Amadeus Basin are less negative than ε_{Nd} values of comparable units from this study. The difference in ε_{Nd} arises from the fact that Gawler Craton derived sediments will have a more negative ε_{Nd} value than sediment derived from the Arunta Block which has a more juvenile ε_{Nd} evolutionary trend (e.g. Zhao et al., 1992; Barovich and Foden, 2000).

ε_{Nd} values of sedimentary rocks located closer to the Gawler Craton than the Musgrave Block would be expected to be more negative than the same sequence more proximal to the Musgrave Block. Of the four formations used in this part of the study, samples of the two younger formations (Relief Sandstone and Observatory Hill Formation) from drillholes closer to the Gawler Craton have a more negative ε_{Nd} value than samples from drillholes further north. However, samples from the two older formations (Murnaroo Formation and Dey Dey Mudstone), do not exhibit this trend. There are a few possible explanations for these differences. Firstly it is possible that this inconsistency is due to the complex nature of the basin architecture (e.g. Leven and Lindsay, 1992). Topographic highs in the basin may have acted as barriers to sediment transport, inhibiting the contribution to a part of the basin by the one source region, but allowing the other source region to dominate the sedimentary input to that region. Alternatively, it is also possible that the Murnaroo Formation and Dey Dey Mudstone are from a period of wide foreland development in the basin, in which much of the eastern Officer Basin was blanketed by sediment shed from the Musgrave Block uplifted during the Petermann Orogeny.

However, as the sample pairs are within error of each other, it could also be argued that the initial ε_{Nd} values represent a mature rock formed from good mixing of source components. If this is the case, the Nd isotope data in this study cannot be used in this way to observe changes in sediment input from proximal and distal sources.

7. Tectonic Implications

The Neoproterozoic to Cambrian intracratonic Petermann Orogeny was a major deformational event, and was responsible for shaping much of the lithospheric architecture of southern Australia, including the Officer Basin. The Petermann Orogeny created some of the largest gravity gradients seen in continental lithosphere.

The Petermann Orogeny overprinted Mesoproterozoic granulite and amphibolite facies gneisses of the Musgrave Block at around 550 Ma, and produced large scale east-west trending shear zones that accommodated dextral strike-slip and north and south directed thrusting (Fig. 8a, Camacho and McDougall, 2000). These shear zones formed under high-*P* amphibolite to transitional eclogite facies conditions (*T*~650°C and *P*~12 kbars; Camacho et al., 1997; Scrimgeour and Close, 1999). The high-pressure Petermann metamorphic terrain appears to have begun exhumation around 550 Ma (Scrimgeour and Close, 1999; Camacho and McDougall, 2000).

Data from this study can be used to test two models for the initiation and duration of the Petermann Orogeny. The ε_{Nd} data from sedimentary rocks in the eastern Officer Basin strongly suggests that the onset of exhumation of the Musgrave Block began at around 640 Ma. This interpretation is similar to that proposed by Shaw (1991) and Calver and Lindsay (1998). Both of these studies argued for dramatic changes in the basin architecture and major uplift of the Musgrave Block around 650-640 Ma. It is known that uplift of the Musgrave Block must have ceased by the early Ordovician (*ca.* 490 Ma), as it is unconformably overlain by early Ordovician units in the Amadeus Basin (Wells et al., 1970; Shaw, 1991).

What is puzzing is why another major Musgrave Block type signal in the Nd isotopic system is not seen in the interval 580-500 Ma, during which up to 40 km of crustal section was exhumed in the northern half of the Musgrave Block (Camacho et al, 1997; Scrimgeour and Close, 1999; Camacho and McDougall, 2000). The relatively subdued input of Musgrave-derived sediments into the eastern Officer Basin over the interval *ca.* 580-500 Ma despite massive denudation of the Musgrave Block implies the existence of a long-lived barrier that prevented sediment input into the eastern Officer Basin. The apparent duration of the barrier (>50 Ma) during the Petermann Orogeny strongly implies that it was maintained by on-going

tectonic processes, that are logically limited to the on-going evolution of the Petermann Orogeny. Several possible scenarios are outlined below:

1) Initial uplift of the northern half of the Musgrave Block occurred around *ca.* 640 Ma, providing an influx of sediment into the eastern Officer Basin as seen by the major excursion in ε_{Nd} values. During a second uplift event at *ca* 550 Ma, uplift was focussed in the northern half of the Musgrave Block. During this time the southern half was incorporated into a foreland basin, trapping sediments shed off the northern part of the Musgrave Block (Fig 8b). In this scenario, sediment was transported northwards into the Amadeus Basin, and deposited in the Carmichael, Mount Currie, and Ooraminna sub-basins as the Arumbera Sandstone and equivalents (Fig. 8b, Korsch and Lindsay, 1989; Shaw, 1991). Sediment derived from erosion of the northern half of the Musgrave Block during this renewed uplift event would have been barred from entering the eastern Officer Basin by the slightly uplifted foreland bulge present in the southern half of the Musgrave Block (e.g. Beaumont, 1981). As a result, sediment eroding from both the northern Musgrave Block and the foreland bulge filled the foreland in the southern margin. Minor erosion of the foreland bulge would also explain the minor contribution to the ε_{Nd} signal from a Musgrave Block type source in the eastern Officer Basin. Transport of sediments out of this foreland basin may have been eastwards along the strike-slip Mann Fault system. Deposition into micro basins such as the Levinger and Moorilyanna grabens would have occurred as eastwards transport of sediment continued (Fig. 8a, e.g. Major and Conor, 1993). Further transport of sediment out of the Petermann Orogen and south-eastwards into the Adelaide Fold Belt could account for the presence of 1100 Ma Musgrave type detrital zircons found in Petermann aged sedimentary rocks such as the Bonney Sandstone in the Adelaide Fold Belt (Fig. 9, Ireland et al., 1998). Possible inversion of the foreland basin in the southern Musgrave Block during the mid- Paleozoic Alice Springs Orogeny (*ca.* 360 Ma, e.g. Haines et al., 2001) would have caused a major influx of this Petermann derived sediment into the eastern Officer Basin. Since sampling did not extend to the Devonian section, this potential influx of Musgrave-derived sediments was not seen in the ε_{Nd} values.

2) Another possibility is that at *ca.* 640 Ma there was uplift of the entire Musgrave Block, shedding sediments into the eastern Officer Basin creating the excursion in ε_{Nd} values. Sediments also shed north into the Amadeus Basin and deposited in depocentres such as

the Carmichael, Mount Currie, and Ooraminna sub-basins (Fig. 8b, e.g. Shaw, 1991). During a second uplift event at *ca.* 540 Ma the northern half of the Musgrave Block underwent major uplift, while the southern half remained slightly uplifted as a result of

the first uplift event at 640 Ma. The southern half acted as a slight topographic high that prevented northern Musgrave Block derived sediment from entering the eastern Officer Basin. Instead, sediment derived from the northern Musgrave Block travelled eastwards along fault systems within the Musgrave Block (Fig. 8a).

Another possibility for the reduced contribution of 580-500 Ma Musgrave derived sediment is sampling restrictions. Due to the scarcity of drillholes in the Officer Basin, it may simply be that the sampled drillholes do not intersect syn-orogenic sediments in the eastern Officer Basin derived from the Musgrave Block. The Arumbera Sandstone in the Amadeus Basin is the sediment associated with the *ca.* 550 Ma exhumation event proposed by Camacho and McDougall (2000). The Arumbera Sandstone does not encompass the entire Amadeus Basin, but is confined to relatively restricted parts of the basin such as the Carmichael, Mount Currie, and Ooraminna sub-basins (Fig 8b). Although Figure 1 does not show the location of all drill-holes within the basin, there are significant parts of the eastern Officer Basin that were not sampled in this study due to government imposed restrictions. Thus it is possible that there is sediment derived from the major *ca.* 550 Ma Petermann uplift event present in the eastern Officer Basin, but is not seen in the isotopic data simply because the sampling locations did not intersect the syn-orogenic sediment shed from this *ca.* 550 Ma uplift event.

8. Conclusions

1) Geochemical and isotopic data from mid-Neoproterozoic to mid-Palaeozoic sedimentary rocks in the eastern Officer Basin define the evolving provenance roles of the Archaean-Mesoproterozoic Gawler Craton, and Mesoproterozoic Musgrave Block. Nd isotopic data from sedimentary rocks in the eastern Officer Basin indicate that the Gawler Craton was the dominant source until around 640 Ma, when there was a dramatic shift to a Musgrave Block dominated sediment source. This dramatic shift was accompanied by an approximate correlation between ε_{Nd} and Sc, Cr, V, and Sc, which is interpreted to reflect erosion of large mafic complexes within the Musgrave Block.

2) The large influx of Musgrave Block-derived sediment at around 640 Ma is interpreted to mark the beginning of the intracratonic Petermann Orogeny, which separated the Officer Basin from the remainder of the Centralian Superbasin, and exhumed the Musgrave Block. Together with existing thermochronologic data from the Petermann Orogen (Camacho et al., 1997; Camacho and McDougall, 2000), the sedimentary provenance data from the eastern Officer Basin indicates that the Petermann Orogeny was either a long-lived event, or series of events that spanned greater than 100 Ma.

3) Despite large regions of the Musgrave Block undergoing around 40-45 km of denudation during the latest Neoproterozoic to early Cambrian, the isotopic compositions of eastern Officer Basin sediments from around 600 Ma onwards suggests that the sediments were increasingly derived from the Gawler Craton. This provenance trend away from the Musgrave Block and toward Gawler Craton sources may reflect the existence of a long-lived barrier that inhibited sediment influx into the southern foreland of the Petermann Orogen.

Acknowledgements

David Bruce and John Stanley are thanked for their invaluable assistance in the laboratory. Thanks go to PIRSA and the staff at the core library for their efficient and quick manner in providing the drill-core. Martin Lee is thanked for his constructive reviews on the manuscript.

References

Anderson, C., Samson, S.D., 1995. Temporal changes in Nd isotopic composition of sedimentary rocks in the Sevier and Taconic foreland basins: Increasing influence of juvenile sources. *Geology*, 23: 983-986.

Barovich, K.M., Foden, J., 2000. A Neoproterozoic flood basalt province in southern-central Australia: geochemical and Nd isotope evidence from basin fill. *Precambrian Research,* 100: 213-234.

Beaumont, C., 1981. Foreland Basins. *Geophysical Journal of the Royal Astronomical Society,* 65: 291-329.

Benbow, M.C., 1982. Stratigraphy of the Cambrian-?Early Ordovician Mount Johns Range. NE Officer Basin, South Australia. *Royal Society of South Australia. Transactions*, 106: 191-211.

Boghossian, N.D., Patchett, P.J., Ross, G.M., Gehrels, G.E., 1996. Nd isotopes and the Source of Sediments in the Miogeocline of the Canadian Cordillera. *Journal of Geology,* 104: 259-277.

Brewer, A.M., Dunster, J.N., Gatehouse, C.G., Henry, R.L., Weste, G., 1987. A revision of the stratigraphy of the eastern Officer Basin. *South Australia. Geological Survey. Quarterly Geological Notes*, 102: 2-15.

Caggianelli, A., Fiore, S., Mongelli, G., Salvemini, A., 1992. REE distribution in the clay fraction of pelites from the southern Apennines, Italy. *Chemical Geology,* 99: 253-263.

Calver, C.R., Lindsay, J.F., 1998. Ediacarian sequence and isotope stratigraphy of the Officer Basin, South Australia. *Australian Journal of Earth Sciences*, 45: 513-532.

Camacho. A., Compston, W., McCulloch, M., McDougall. I., 1997. Timing and exhumation of eclogite facies shear zones, Musgrave Block, central Australia. *Journal of Metamorphic Geology*, 15: 735-751.

Camacho, A., McDougall, I., 2000. Intracratonic, strike-slip partitioned transpression and the formation and exhumation of eclogite facies rocks: An example from the Musgrave Block, central Australia. *Tectonics*, 19: 978-996.

Creaser, R.A., 1995. Neodymium isotopic constraints for the origin of Mesoproterozoic felsic magmatism, Gawler Craton, South Australia. *Canadian Journal of Earth Sciences*, 32: 460-471.

Crichton, J.G., Condie, K.C., 1993. Trace elements as source indicators in cratonic sediments: a case study from the early Proterozoic Libby Creek Group, southeastern Wyoming. *Journal of Geology*, 101: 319-332.

Dabard, M.P., Loi, A., Peucat, J.J., 1996. Zircon typology combined with Sm-Nd whole-rock isotope analysis to study Brioverian sediments from the Amorican Massif. *Sedimentary Geology,* 101: 243-260.

Daly, S.J., Fanning, C.M., Fairclough, M.C., 1998. Tectonic evolution and exploration potential of the Gawler Craton, South Australia. *AGSO Journal of Australian Geology & Geophysics,* 17: 145-168.

Dunster, J.N., 1987. Sedimentology of the Ouldburra Formation (Early Cambrian) northeastern Officer Basin. *University of Adelaide. M.Sc. thesis (unpublished).*

Garzione, C.N., Patchett, P.J., Ross, G.M., Nelson, J., 1997. Provenance of Paleozoic sedimentary rocks in the Canadian Cordilleran miogeiocline: a Nd isotopic study. *Canadian Journal of Earth Sciences,* 34: 1603-1618.

Gatehouse, C.G., Benbow, M.C., Major, R.B., 1986. The Murnaroo Formation of the Officer Basin. *South Australia. Geological Survey. Quarterly Geological Notes*, 97: 17-20.

Glikson, A.Y., Ballhaus, C.G., Clarke, G.L., Sheraton, J.W., Stewart, A.J., Sun, S-S., 1996. Geological framework and crustal evolution of the Giles mafic-ultramafic complex and environs, western Musgrave Block, central Australia. *AGSO Journal of Australian Geology and Geophysics,* 16: 41-67.

Gravestock, D.I., 1997. Geological Setting and Structural History. In: J.G.G. Morton (Ed.) and J.F. Drexel (Ed.), The Petroleum Geology of South Australia, Vol.3: Officer Basin, ch.6, pp 47-86.

Haines, P.W., Hand, M., Sandiford, M., 2001. Palaeozoic syn-orogenic sedimentation in central and northern Australia: a review of distribution and timing with implications for the evolution of intracontinental orogens. *Australian Journal of Earth Sciences, in press*.

Hand, M., Sandiford. M, 1999. Intraplate deformation in central Australia, the link between subsidence and fault reactivation. *Tectonophysics*, 305: 121-140.

Hoskins, D., Lemon, N., 1995. Tectonic development of the eastern Officer Basin, central Australia. *Exploration Geophysics*, 26: 395-402.

Ireland, T.R., Flöttmann, T., Fanning, C.M., Gibson, G.M., Preiss, W.V., 1998. Development of the early Paleozoic Pacific margin of Gondwana from detrital-zircon ages across the Delamerian Orogen. *Geology*, 26: 243-246.

Jago, J.B., Tian-rui Lin, Dunster, J.N., 1994. Early Cambrian trilobites from the Ouldburra Formation, Manya 6, eastern Officer Basin. *PESA Journal*, 22: 87.

Jago, J.B., Youngs, B.C., 1980. Early Cambrian trilobites from the Officer Basin, South Australia. *Royal Society of South Australia. Transactions*, 104: 197-199.

Jenkins, R.J.F., McKirdy, D.M., Foster, C.B., O'Leary, T., Pell, S.D., 1992. The record and stratigraphic implications of organic-walled microfossils from the Ediacaran (terminal Proterozoic) of South Australia. *Geological Magazine*, 129: 401-410.

Korsch, R.J., Lindsay, J.F., 1989. Relationships between deformation and basin evolution in the intracratonic Amadeus Basin, central Australia. *Tectonophysics*, 158: 5-22.

Korsch, R.J., Goleby, B.R., Leven, J.H., Drummond, B.J., 1998. Crustal architecture of central Australia based on deep seismic reflection profiling. *Tectonophysics*, 288: 57-69.

Leven, J.H., Lindsay, J.F., 1992. Morphology of the Late Proterozoic to Early Palaeozoic Officer Basin, South Australia. *Exploration Geophysics,* 23: 191-196.

Li, X., McCulloch, M.T., 1996. Secular variation in the Nd isotopic composition of Neoproterozoic sediments from the southern margin of the Yangtze Block: evidence for a Proterozoic continental collision in southeast China. *Precambrian Research*, 76: 67-76.

Lindsay, J.F., 1987. Sequence stratigraphy and depositional controls in late Proterozoic-Early Cambrian sediments of Amadeus Basin, central Australia. *AAPG Bulletin*. 71: 1387-1403.

Lindsay, J.F., Leven, J.H., 1996. Evolution of a Neoproterozoic to Palaeozoic intracratonic setting, Officer Basin, South Australia. *Basin Research*, 8: 403-424.

Long, J.A., Turner, S., Young, G.C., 1988. A Devonian fish fauna from subsurface sediments in the eastern Officer Basin, South Australia. *Alcheringa*, 12: 61-78.

Major, R.B., Conor, C.H.H., 1993. Musgrave Block. In: *The Geology of South Australia, Vol.1, the Precambrian* (Ed. by J.F. Drexel, W.V. Preiss and A.J. Parker) *Bulletin of Geological Survey, South Australia*, 54: 156-167.

McCulloch, M.T., Wasserburg, G.J., 1978. Sm-Nd and Rb-Sr chronology of continental crust formation. *Science*, 200: 1003-1011.

McLennan, S.M., 1989. Rare earth elements in sedimentary rocks: influence of provenance and sedimentary processes. In: B.R. Lipin and G.A. McKay (Ed.), Geochemistry and Mineralogy of Rare Earth Elements. Am. Mineral. Soc., *Rev. Mineral.*, 21: 169-200.

McLennan, S.M., Taylor, S.R., 1982. Geochemical constraints on the growth of the continental crust, *Journal of Geology,* 90: 347-361.

McLennan, S.M., McCulloch, M.T., Taylor, S.R., Maynard, J.B., 1989. Effects of sedimentary sorting on neodymium isotopes in deep sea turbidites. *Nature*, 337: 547-549.

McLennan, S.M., Taylor, S.R., McCulloch, M.T., Maynard, J.B., 1990. Geochemical and Nd-Sr isotopic composition of deep sea turbidites: Crustal evolution and plate tectonic associations. *Geochimica et Cosmochimica Acta* 54: 2015-2050.

McLennan, S.M., Hemming, S., McDaniel, D.K., Hanson, G.N., 1993. Geochemical approaches to sedimentation, provenance, and tectonics. *Geological Society of America, Special Paper*, 284: 21-40.

Morton, J.G.G., 1997. Lithostratigraphy and environments of deposition. In: J.G.G. Morton (Ed.) and J.F. Drexel (Ed.), The Petroleum Geology of South Australia, Vol.3: Officer Basin, ch.6: pp 47-86.

Moussavi-Harami, R., Gravestock, D.I., 1995. Burial history of the eastern Officer Basin, South Australia. *APEA Journal* 35: 307-320.

Neumann, N.L., 2001. Geochemical and isotopic characterisitcs of South Australian Proterozoic granites: Implications for the origin and evolution of high heat-producing terrains. *Adelaide University (South Australia). Ph.D. thesis.*

Parker, A.J., Lemon, M.N., 1982. Reconstruction of the Early Proterozoic stratigraphy of the Gawler Craton, South Australia. *Journal of the Geological Society of Australia*, 29: 221-238.

Pell, S.D., McKirdy, D.M., Jansyn, J., Jenkins, R.J.F., 1993. Ediacaran carbon isotope stratigraphy of South Australia- an initial study. *Royal Society of South Australia. Transactions*, 117: 153-161.

Plumb, K.A, 1985. Subdivision and correlation of the late Precambrian sequences in Australia. *Precambrian Research,* 29: 303-329.

Prame W.K.B.N., Pohl J., 1994. Geochemistry of pelitic and psammopelitic Precambrian metasediments from southwestern Sri Lanka: implications for two contrasting source-terrains and tectonic settings: *Precambrian Research*, 66: 223-244.

Preiss W.V., 1973. Early Willouran stromatolites from the Peake and Denison Ranges and their stratigraphic significance. *South Australia. Department of Mines and Energy. Report Book*, 73/208.

Preiss, W.V., 1987. The Adelaide Geosyncline-Late Proterozoic stratigraphy, sedimentation, palaeontology and tectonics. *South Australia. Geological Survey. Bulletin*, 53.

Preiss, W.V., 1993. Neoproterozoic. In: Drexel, J.F., Preiss, W.V., Parker, A.J., The geology of South Australia. Vol. 1, The Precambrian. *South Australia. Geological Survey. Bulletin*, 54: 171-203.

Preiss, W.V., 2000. The Adelaide Geosyncline of South Australia and its significance in the Neoproterozoic continental reconstruction. *Precambrian Research,* 100: 21-63.

Preiss, W.V., Forbes, B.G., 1981. Stratigraphy, correlation and sedimentary history of Adelaidean (Late Proterozoic) basins in South Australia. *Precambrian Research,* 15: 255-304.

Rankin, L.R., Martin, A.R., Parker, A.J., 1989. Identification of a major crustal shear zone, northwest Gawler Craton, South Australia. *Australian Journal of Earth Sciences*, 36: 123-133.

Schaefer, B.F., 1998. Insights into Proterozoic tectonics from the southern Eyre Peninsula, South Australia. *Adelaide University (South Australia). Ph.D. thesis*.

Scrimgeour, I., Close, D., 1999. Regional high-pressure metamorphism during intracratonic deformation; the Petermann Orogeny, central Australia. *Journal of Metamorphic Geology*, 17: 557-572.

Shaw, R.D., 1991. The tectonic development of the Amadeus Basin, central Australia. *Bulletin Bureau of Mineral Resources, Australia, Canberra, A.C.T.,* 236: 447-476.

Shaw, R.D., Black, L.P., 1991. The history and tectonic implications of the Redbank thrust zone, central Australia, based on structural, metamorphic and Rb-Sr isotopic evidence. *Australian Journal of Earth Sciences,* 38: 307-332.

Slack, J.F., Stevens, B.P.J., 1994. Clastic metasediments of the Early Proterozoic Broken Hill Group, New South Wales, Australia: Geochemistry, provenance, and metallogenic significance. *Geochimica et Cosmochimica,* Acta 58: 3633-3652.

Stainton, P.W., Weste, G., Cucuzza, G., 1988. Exploration of PEL 23 and PEL 30, eastern Officer Basin, South Australia, 1983-1988. *South Australia. Department of Mines and Energy Resources. Open file Envelope*, 5073: 1243-1321.

Sukanta, U., 1993. Sedimentology, sequence stratigraphy and palaeogeography of Marinoan sediments in the eastern Officer Basin, South Australia. *Flinders University (South Australia). Ph.D. thesis (unpublished).*

Taylor S.R., McLennan S.M., 1985, The Continental Crust: its composition and Evolution. Blackwell, Oxford.

Turner, S., Foden, J., Sandiford, M., Bruce, D., 1993. Sm-Nd isotopic evidence for the provenance of sediments from the Adelaide Fold Belt and southeastern Australia with implications for episodic crustal addition. *Geochimica et Cosmochimica,* Acta 57: 1837-1856.

Ugidos J.M., Valladares M.I., Recio C., Rogers G., Fallick A.E., Stephens W.E., 1997. Provenance of Upper Precambrian-Lower Cambrian shales in the Central Iberian Zone, Spain: evidence from a chemical and isotopic study. *Chemical Geology*, 136: 55-70.

Walter, M.R., Veevers, J.J., Calver, C.R., Grey, K., 1995. Neoproterozoic stratigraphy of the Centralian Superbasin, Australia. *Precambrian Research,* 73: 173-195.

Wells, A.T., Forman, D.J., Ranford, L.C., Cook, P.J., 1970. Geology of the Amadeus Basin, central Australia. *Bulletin- Australia, Bureau of Mineral Resources, Geology and Geophysics,* 100: pp216.

Wingate, M.T.D., Campbell, I.H., Compston, W., Gibson, G.M., 1998. Ion microprobe U-Pb ages for Neoproterozoic basaltic magmatism in south-central Australia and implications for the breakup of Rodinia. *Precambrian Research,* 87: 135-159.

Womer, M.B., Baker, R.N., Newman, E.J., van Nieuwenhuise, R., 1987. Technical evaluation of PEL 29, east Officer Basin, Australia. Report for Amoco Australia Production Company. *South Australia. Department of Mines and Energy Resources. Open file Envelope*, 6843 (unpublished).

Young, D., Duncan, N., Sheraton, J., Sun, S-S., Comacho, A., 1998. Metallogenic Potential of Australian Proterozoic Granites. *AGSO Presentation Material Volume*, pp 139-144.

Zang, W-L, 1994. Review of Neoproterozoic and Early Palaeozoic acritarch biostratigraphy in Australia. *PESA Journal*, 22: 101-106.

Zang, W-L, 1995. Early Neoproterozoic sequence stratigraphy and acritarch biostratigraphy, eastern Officer Basin, South Australia. *Precambrian Research,* 74: 119-175.

Zhao, J.X., McCulloch, M.T., Bennett, V.C., 1992. Sm-Nd and U-Pb zircon isotopic constraints on the provenance of sediments from the Amadeus Basin, central Australia: evidence for REE fractionation. *Geochimica et Cosmochimica*, *Acta* 56: 921-940.

Table 1

Sample types (from this study) and localities

Officer Basin Sample #	Unit	Sample Type	Locality	Est. Age[a] (Ma)
474608	Munda Group - Blue Hills Sandstone	sandstone	Lairu 1	443
474609	Munda Group - Indulkana Shale	sandstone	Lairu 1	450
474611	Munda Group - Mount Chandler Sandstone	sandstone	Lairu 1	475
474612	Munda Group - Mount Chandler Sandstone	sandstone	Lairu 1	475
474613	Marla Group - Trainor Hill Sandstone	sandstone	Lairu 1	513
474614	Marla Group - Trainor Hill Sandstone	sandstone	Lairu 1	513
474615	Marla Group - Trainor Hill Sandstone	sandstone	Lairu 1	513
474620	Marla Group - Apamurra Formation	mudstone	Karlaya 1	517
473831	Marla Group - Arcoeillinna Sandstone	mudstone	Karlaya 1	519
473902	Marla Group - Observatory Hill Formation	mudstone	Observatory Hill 1	522
474616	Marla Group - Observatory Hill Formation	shale	Marla 3	522
473904	Marla Group - Relief Sandstone	sandstone	Observatory Hill 1	530
473827	Marla Group - Relief Sandstone	sandstone	Meramangye 1	530
473833	Ungoolya Group - Mena Mudstone Member	mudstone	Karlaya 1	560
480260	Ungoolya Group - Tanana Formation	mudstone	Karlaya 1	580
480261	Ungoolya Group - Tanana Formation	mudstone	Karlaya 1	580
480262	Ungoolya Group - Tanana Formation	sandstone	Karlaya 1	580
480266	Ungoolya Group - Dey Dey Mudstone	mudstone	Karlaya 1	595
473910	Ungoolya Group - Dey Dey Mudstone	mudstone	Murnaroo 1	595
473990	Lake Maurice Group - Murnaroo Formation	shale	Munta 1	620
473991	Lake Maurice Group - Murnaroo Formation	sandstone	Munta 1	620
473992	Lake Maurice Group - Murnaroo Formation	mudstone	Munta 1	620
474014	Lake Maurice Group - Murnaroo Formation	sandstone	Lake Maurice East 1	620
474015	Lake Maurice Group - Murnaroo Formation	mudstone	Lake Maurice East 1	620
474018	Lake Maurice Group - Murnaroo Formation	sandstone	Lake Maurice East 1	620
473997	Lake Maurice Group - Meramangye Fmtn	siltstone	Giles 1	635
474001	Lake Maurice Group - Tarlina Sandstone	sandstone	Giles 1	645
474005	Callanna Group - Alinya Formation	dol. siltstone	Giles 1	790
474008	Callanna Group - Pindyin Sandstone	sandstone	Giles 1	810

[a] Ages from Dunster, (1987), Jago and Youngs, (1980), Jago et al., (1994), Jenkins et al. (1992), Long et al., (1988), Pell et al., (1993), Preiss, (1973, 1987, 1993), Womer et al. (1987), Zang, (1994, 1995)

Table 2

Major and trace element data for Officer Basin samples (from this study)

	Officer Basin																										
Stratigraphy	Pindyin Sst	Alinya Fmtn	Tarlina Sst	Meramangye	Murnaroo	Murnaroo	Murnaroo	Murnaroo	Murnaroo	Murnaroo	Dey Dey	Dey Dey	Tanana Fmtn	Tanana Fmtn	Tanana Fmtn	Mena Mudst	Relief sst	Relief sst	Observatory Hill	Observatory Hill	Arcoeillinna sst	Apamurra Fmtn	Trainor Hill Sst	Trainor Hill Sst	Trainor Hill Sst	Mt Chandler Sst	Mt Chandler Sst	Indulkana Shale	Blue Hills Sst
	(Sst)	(dol. Sltstn)	(Sst)	Fmtn (Slst)	Fmtn (Sst)	Fmtn (Mdst)	Fmtn (Sst)	Fmtn (Shale)	Fmtn (Sst)	Fmtn (Mdst)	Mdst (Mdst)	Mdst (Mdst)	(Mdst)	(Mdst)	(Mdst)	Mbr (Mdst)	(Sst)	(Sst)	Fmtn (Shale)	Fmtn (Mdst)	(Mdst)	(Mdst)	(Sst)	(Sst)	(Sst)	(Sst)	(Sst)	(Sst)	(Sst)
Sample no.	2012-008	2012-005	2012-001	2012-997	2012-014	2012-015	2012-018	2012-990	2012-991	2012-992	2012-266	2012-910	2012-260	2012-261	2012-262	2012-833	2012-827	2012-904	2012-616	2012-902	2012-831	2012-620	2012-613	2012-614	2012-615	2012-611	2012-612	2012-609	2012-608
SiO2	98.70	19.46	80.13	66.56	95.96	66.00	89.78	57.25	78.92	67.50	62.68	59.62	62.82	62.33	60.38	57.39	96.11	82.65	54.77	64.50	55.10	56.73	88.71	85.03	79.83	97.80	99.29	91.24	99.89
Al2O3	0.58	3.49	7.27	11.82	1.58	9.38	3.53	16.34	6.94	10.57	13.78	15.23	10.70	12.65	13.08	12.76	1.65	5.86	16.55	12.92	17.13	14.01	4.10	5.19	5.13	1.02	0.24	2.97	0.15
Fe2O3 (T)	0.07	0.96	2.51	5.87	0.28	4.82	1.30	9.17	5.28	8.78	7.76	8.45	5.40	5.98	6.78	5.52	0.24	0.31	8.20	5.31	9.68	6.33	1.87	3.13	6.14	0.47	0.22	1.63	0.11
MnO	0.00	0.39	0.06	0.12	0.00	0.11	0.00	0.09	0.02	0.03	0.10	0.11	0.08	0.09	0.10	0.12	0.00	0.01	0.05	0.07	0.11	0.14	0.16	0.08	0.07	0.00	0.00	0.01	0.00
MgO	0.02	16.17	1.14	2.64	0.06	4.04	0.26	3.56	0.84	1.60	3.48	3.34	3.65	4.08	4.32	4.06	0.07	1.04	6.71	2.75	5.35	5.13	0.25	0.30	0.51	0.04	0.01	0.28	0.01
CaO	0.02	22.36	1.18	1.87	0.03	3.10	0.03	0.78	0.36	0.46	1.18	0.88	4.32	2.45	2.41	5.93	0.05	1.74	1.01	2.76	0.43	3.22	0.07	0.12	0.17	0.02	0.01	0.05	0.02
Na2O	0.00	0.20	1.56	2.05	0.11	1.31	0.25	1.03	1.33	1.73	1.77	1.50	2.70	2.39	1.62	1.51	0.10	0.36	0.93	2.86	1.74	0.98	0.13	0.14	0.17	0.02	-0.01	0.15	-0.01
K2O	0.16	1.39	2.36	2.82	1.18	3.32	1.87	4.94	2.87	3.58	3.68	5.09	2.79	3.15	3.68	3.53	1.24	4.52	4.81	3.13	4.63	5.02	2.80	3.84	3.60	0.07	0.02	0.58	0.01
TiO2	0.04	0.20	0.47	1.02	0.03	0.78	0.14	1.51	1.30	3.08	0.84	0.85	0.66	0.70	0.75	0.66	0.04	0.10	0.62	0.75	0.91	0.79	0.16	0.25	0.37	0.06	0.03	0.14	0.02
P2O5	0.01	0.07	0.07	0.18	0.02	0.12	0.03	0.15	0.10	0.20	0.12	0.13	0.23	0.19	0.14	0.14	0.02	0.04	0.13	0.20	0.16	0.17	0.05	0.08	0.10	0.01	0.01	0.03	0.01
SO3	0.02	0.21	0.08	0.04	0.00	0.05	0.01	0.01	0.01	0.01	0.00	0.01	0.03	0.04	0.05	0.15	0.02	0.31	0.01	0.08	0.01	0.03	0.00	0.00	0.02	0.00	0.00	0.01	0.00
LOI	0.24	35.04	2.45	4.42	0.29	6.34	0.92	4.62	1.73	2.17	4.16	4.10	6.22	5.23	5.98	8.34	0.33	2.56	5.50	4.06	4.43	7.40	1.37	1.71	3.27	0.74	0.32	1.61	0.14
Total (%)	99.86	99.94	99.28	99.41	99.54	99.37	98.11	99.45	99.7	99.70	99.56	99.31	99.60	99.27	99.28	100.11	99.87	99.5	99.28	99.38	99.68	99.94	99.68	99.88	99.40	100.26	100.15	98.72	100.35
Cr (ppm)	7.00	22.00	34.00	67.00	10.00	61.00	10.0	90.00	43.00	61.0	83.0	89.00	65.0	90.0	80.0	84.00	6.00	15.00	114.0	98.0	130.00	103.0	17.0	19.0	23.0	9.0	6.0	33.0	6.0
Ni	1.00	10.00	17.00	29.00	4.00	28.00	3.0	45.00	20.00	35.0	39.0	50.00	23.0	36.0	33.0	35.00	2.00	3.00	53.0	32.0	57.00	37.0	3.0	5.0	6.0	3.0	1.0	6.0	1.0
Sc	0.80	4.10	6.70	12.20	0.40	11.80	2.1	21.10	7.20	15.6	15.8	17.90	12.1	13.0	14.2	14.10	1.20	1.80	15.9	12.3	21.60	15.6	2.5	3.5	4.1	1.1	0.0	4.8	0.6
V	4.00	40.00	58.00	107.00	10.00	117.00	16.0	161.00	160.00	278.0	111.0	128.00	77.0	90.0	100.0	95.00	5.00	7.00	138.0	90.0	106.00	94.0	18.0	21.0	35.0	6.0	3.0	24.0	3.0
Pb	1.50	3.90	9.90	15.60	6.00	19.60	5.1	19.80	18.00	22.4	11.2	30.10	16.5	16.9	8.0	8.60	5.30	18.50	16.9	26.0	32.20	21.6	12.0	22.0	20.6	1.9	1.4	8.9	1.3
Zn	0.00	29.00	16.00	42.00	2.00	45.00	6.0	134.00	29.00	53.0	85.0	86.00	54.0	71.0	85.0	68.00	5.00	8.00	118.0	74.0	115.00	86.0	10.0	7.0	14.0	18.0	3.0	37.0	2.0
Rb	8.10	57.50	88.10	121.00	39.20	103.40	53.4	207.80	104.20	133.7	172.2	193.80	105.4	134.1	159.2	142.50	33.40	122.20	189.4	144.2	206.30	178.1	68.5	121.7	113.0	3.1	1.0	24.9	1.1
Sr	37.30	74.60	74.20	80.40	18.10	59.70	45.1	85.70	104.20	90.2	64.1	79.90	165.9	194.1	215.3	105.40	25.10	92.10	72.9	121.4	65.80	55.6	59.0	47.7	49.5	15.3	7.8	49.2	3.5
Ba	652.00	287.00	496.00	441.00	181.00	312.00	1947.0	356.00	404.00	363.0	435.0	473.00	645.0	824.0	626.0	437.00	234.00	941.00	447.0	701.0	487.00	474.0	555.0	544.0	510.0	21.0	11.0	146.0	13.0
Ga	2.00	5.70	9.20	12.70	2.80	12.70	4.4	23.10	8.30	16.1	18.1	22.00	13.0	15.3	18.8	15.90	2.80	6.30	24.0	17.8	28.30	20.0	4.5	6.4	6.2	2.2	1.6	5.9	2.0
Nb	0.80	2.30	5.10	16.20	1.30	9.20	2.6	21.50	9.60	26.0	15.9	15.20	14.6	16.8	15.6	13.20	0.50	2.50	13.2	16.6	18.60	16.9	3.4	4.6	6.2	0.7	0.8	2.6	1.0
Zr	70.00	61.20	163.90	264.50	21.90	227.30	116.8	324.20	157.90	423.5	194.3	171.80	306.1	202.4	186.5	170.30	51.70	114.30	116.9	346.5	193.40	217.8	128.3	180.9	288.1	147.2	59.3	98.9	43.2
Y	3.00	20.80	13.90	36.50	3.60	24.20	6.7	43.20	16.10	32.8	32.0	32.30	36.5	33.6	31.6	30.00	5.90	6.30	21.7	37.4	34.30	25.0	12.2	20.6	23.9	4.5	2.5	13.3	4.4
Co	189.00	16.00	34.00	21.00	110.00	29.00	119.0	28.00	40.00	33.0	26.0	30.00	23.0	25.0	20.0	22.00	80.00	58.00	24.0	24.0	34.00	32.0	57.0	57.0	45.0	74.0	100.0	36.0	60.0
Th	2.90	7.50	4.20	16.10	1.70	9.90	3.2	24.50	6.90	14.2	21.1	22.00	17.7	18.9	18.2	16.30	1.60	3.40	17.9	22.7	23.80	21.5	7.8	12.0	24.6	2.8	1.7	5.4	1.7
U	-0.20	1.30	1.50	3.60	0.70	2.30	0.7	8.70	0.60	2.6	1.8	3.10	3.8	2.8	2.3	3.70	0.30	-0.50	5.2	5.4	6.80	4.7	0.8	2.0	3.1	0.4	0.7	1.9	0.6
La	14.00	15.00	13.00	33.00	3.00	23.00	7.0	51.00	18.00	36.0	39.0	46.00	44.0	41.0	35.0	36.00	8.00	8.00	45.0	50.0	64.00	43.0	21.0	22.0	31.0	4.0	4.0	14.0	3.0
Ce	27.00	41.00	30.00	69.00	4.00	47.00	18.0	104.00	41.00	79.0	81.0	92.00	91.0	91.0	73.0	74.00	17.00	14.00	96.0	98.0	123.00	75.0	49.0	47.0	73.0	12.0	6.0	26.0	6.0
Nd	10.00	14.00	11.00	28.00	4.00	20.00	8.0	41.00	18.00	30.0	31.0	35.00	42.0	36.0	31.0	31.00	7.00	6.00	38.0	42.0	41.00	34.0	15.0	20.0	29.0	4.0	2.0	12.0	2.0

Abbreviations: Sst=sandstone, dol. Sltstn=dolomitic siltstone, Slst=siltstone, Mdst=mudstone

Table 3

Sm-Nd isotope data for Officer Basin samples (from this study)

Rock	Est. Age (Ma)	Sample no.	Nd (ppm)	Sm (ppm)	$^{147}Sm/^{144}Nd$	$^{143}Nd/^{144}Nd$	2σ[a]	$\varepsilon_{Nd}(0)$	$\varepsilon_{Nd}(t)$	Sample type
Pindyin Sandstone	810	2012-008	9.2	1.2	0.0772	0.511182	32	-28.4	-16.1	sandstone
Alinya Formation	790	2012-005	14.0	1.3	0.1008	0.511591	68	-20.4	-10.8	dolomitic siltstone
Tarlina Sandstone	645	2012-001	12.1	2.5	0.1226	0.511265	70	-26.8	-20.7	sandstone
Meramangye Fmtn	635	2012-997	30.0	6.3	0.1274	0.511883	63	-14.7	-9.1	siltstone
Murnaroo Formation	620	2012-990	40.2	8.0	0.1202	0.511896	17	-15.7	-9.7	shale
Murnaroo Formation	620	2012-015	20.3	4.1	0.1216	0.511992	60	-13.8	-7.8	mudstone
Dey Dey Mudstone	595	2012-266	33.7	6.4	0.1141	0.511759	61	-17.1	-10.9	mudstone
Dey Dey Mudstone	595	2012-910	36.1	6.9	0.1148	0.511777	74	-16.8	-10.6	mudstone
Tanana Formation	580	2012-261	38.4	7.2	0.1133	0.511717	83	-18.0	-11.8	mudstone
Mena Mudstone	560	2012-833	31.8	6.1	0.1152	0.511804	72	-17.4	-11.6	mudstone
Relief sandstone	530	2012-827	7.8	1.5	0.1138	0.511840	90	-16.7	-11.1	sandstone
Relief sandstone	530	2012-904	6.7	1.4	0.1232	0.511804	16	-17.4	-12.4	sandstone
Observatory Hill Fmtn	522	2012-902	41.7	7.7	0.1121	0.511660	77	-19.1	-13.5	mudstone
Observatory Hill Fmtn	522	2012-616	35.9	6.0	0.1012	0.511670	69	-18.9	-12.5	shale
Arcoeillinna sandstone	519	2012-831	41.4	7.6	0.1116	0.511746	80	-18.6	-13.0	mudstone
Apamurra Formation	517	2012-620	38.5	7.0	0.1103	0.511738	77	-17.6	-11.9	mudstone
Trainor Hill Sandstone	513	2012-614	22.9	4.5	0.1193	0.511705	75	-18.2	-13.2	sandstone
Mt Chandler Sandstone	475	2012-612	2.8	0.5	0.1158	0.511690	73	-18.5	-13.6	sandstone
Indulkana Shale	450	2012-609	11.5	2.4	0.1238	0.511691	50	-18.5	-14.3	sandstone

[a] Isotope error measurements are $2\sigma_{mean}$

[b] $^{143}Nd/^{144}Nd_{CHUR(0)} = 0.512638$, $^{147}Sm/^{144}Nd_{CHUR} = 0.1967$, $\lambda = 6.54E\text{-}12$

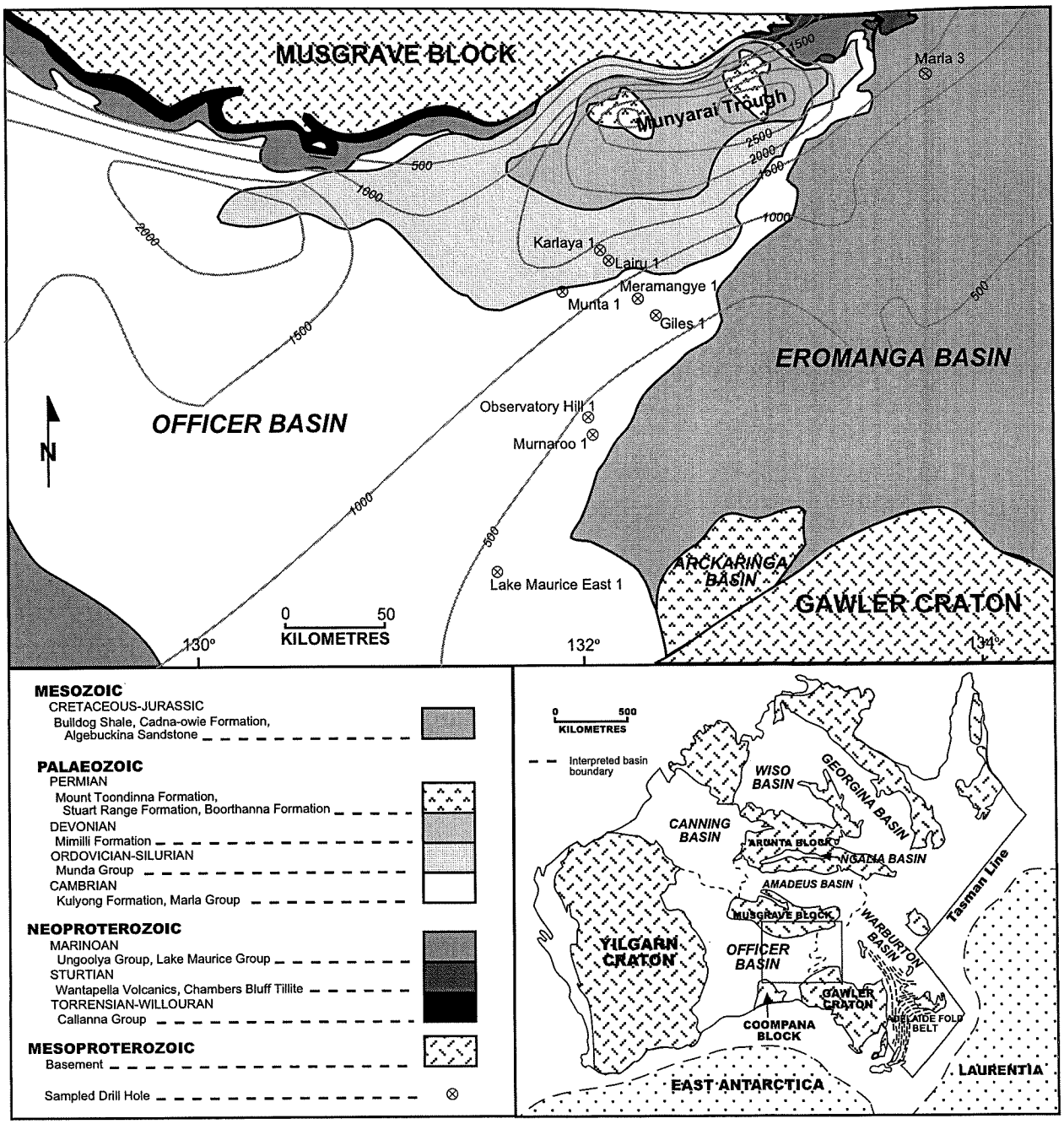

Fig. 1. Map of the Officer Basin in South Australia. Basement complexes that border the basin are: (1) the Mesoproterozoic Musgrave Block to the north, (2) the Archaean-Paleoproterozoic Gawler Craton to the south (adapted from Morton, 1997). Inset: Map of Australia showing the location of basement complexes and basins within Australia (adapted from Gravestock, 1997). Square area represents the part of the Officer Basin that resides in South Australia. The Officer, Amadeus, Canning, Wiso, Georgina, Ngalia, and Warburton Basins formerly comprised the Centralian Superbasin (Walter et al., 1995). Isopach thicknesses in two way time (2 seconds approximately 5 km).

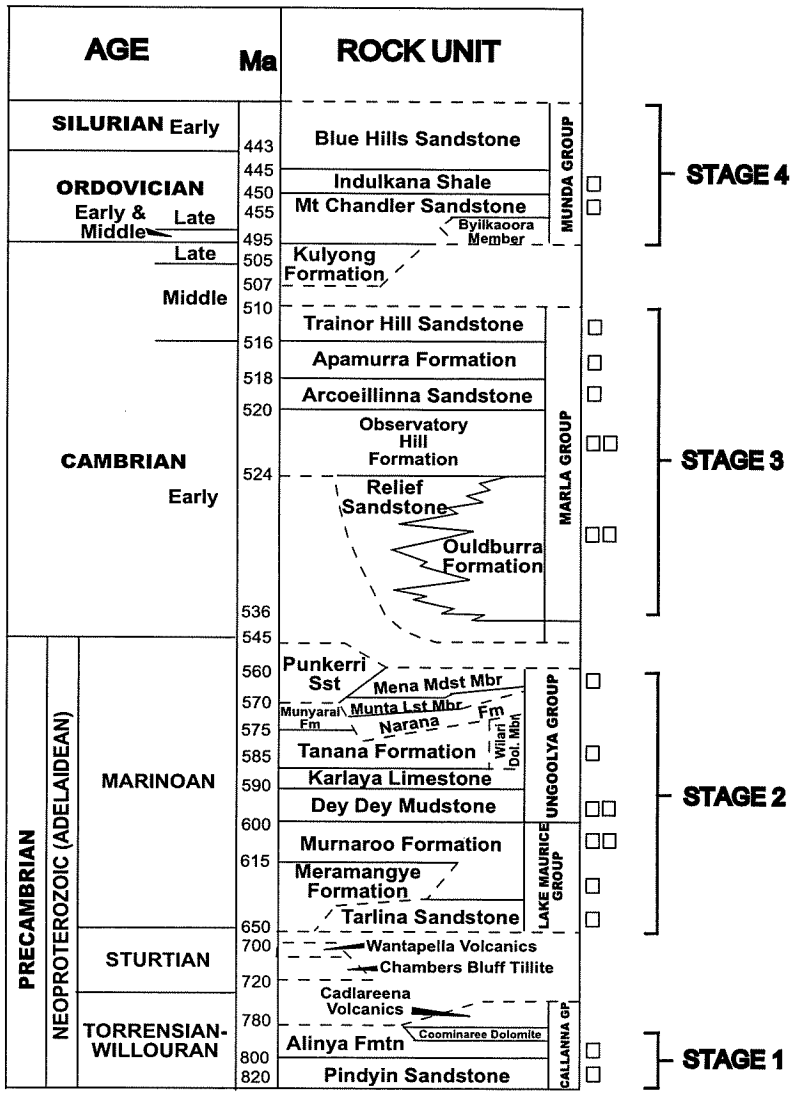

Fig. 2. Simplified stratigraphic column of the Officer Basin successions (adapted from Lindsay and Leven, 1996). Sample locations in this study are shown as square symbols to the right of the unit. The four stages of the evolution of the Officer Basin encompassing the deposition of the relevant sequences are shown to the right of the column & described in the text (Moussavi-Harami and Gravestock, 1995; Hoskins and Lemon, 1995, Lindsay

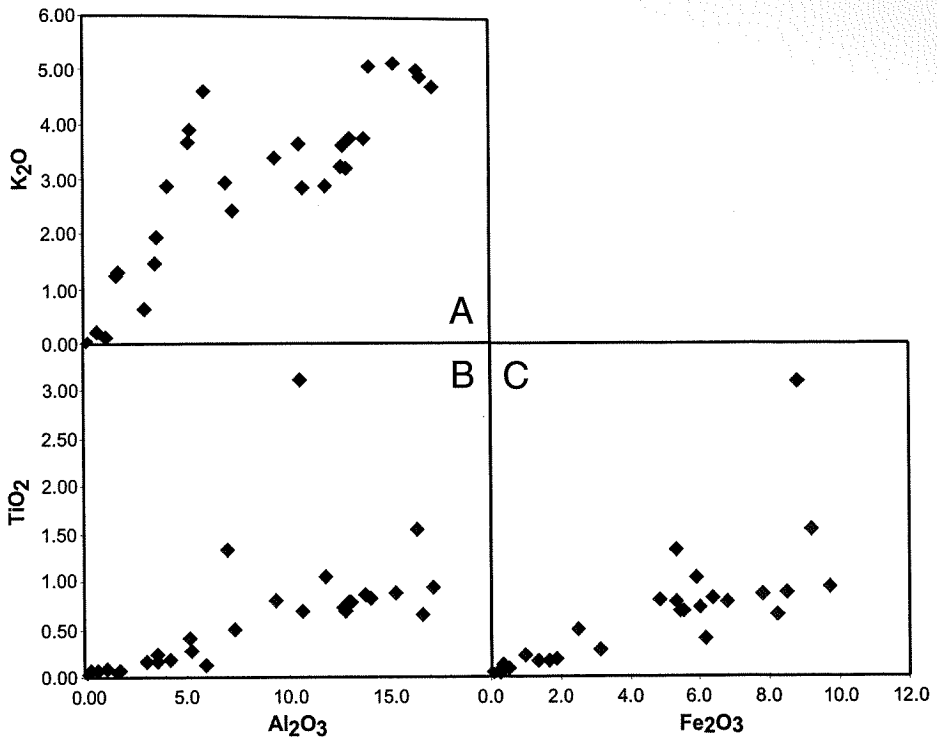

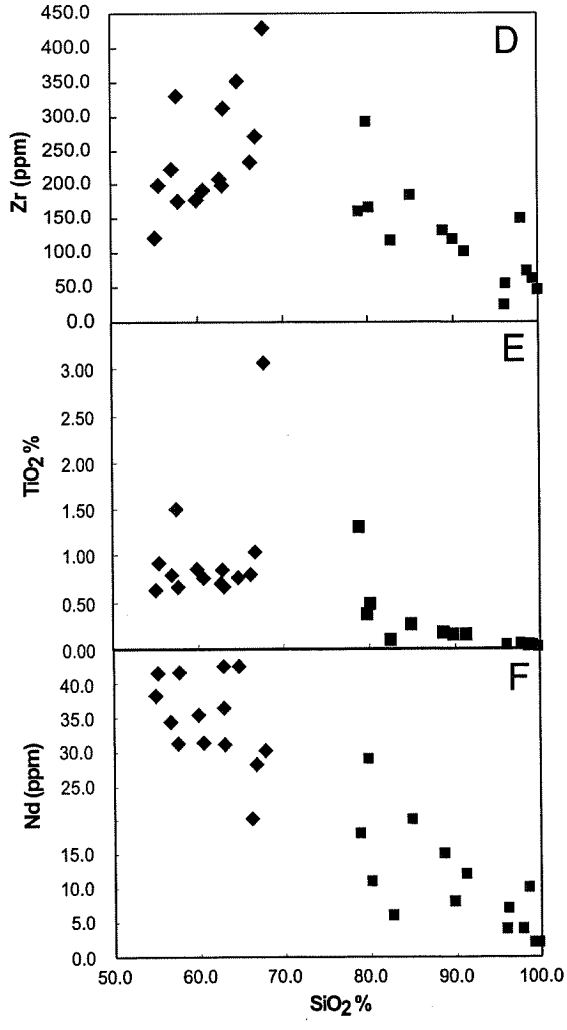

Fig. 3. Major element variation diagrams for Officer Basin sedimentary rocks (filled diamonds). (a) K_2O-Al_2O_3; (b) TiO_2-Al_2O_3; (c) TiO_2-Fe_2O_3. (d-f) Variation of Zr, TiO_2, and Nd vs SiO_2 (squares=sandstones,diamonds=mudstones/ siltstones).

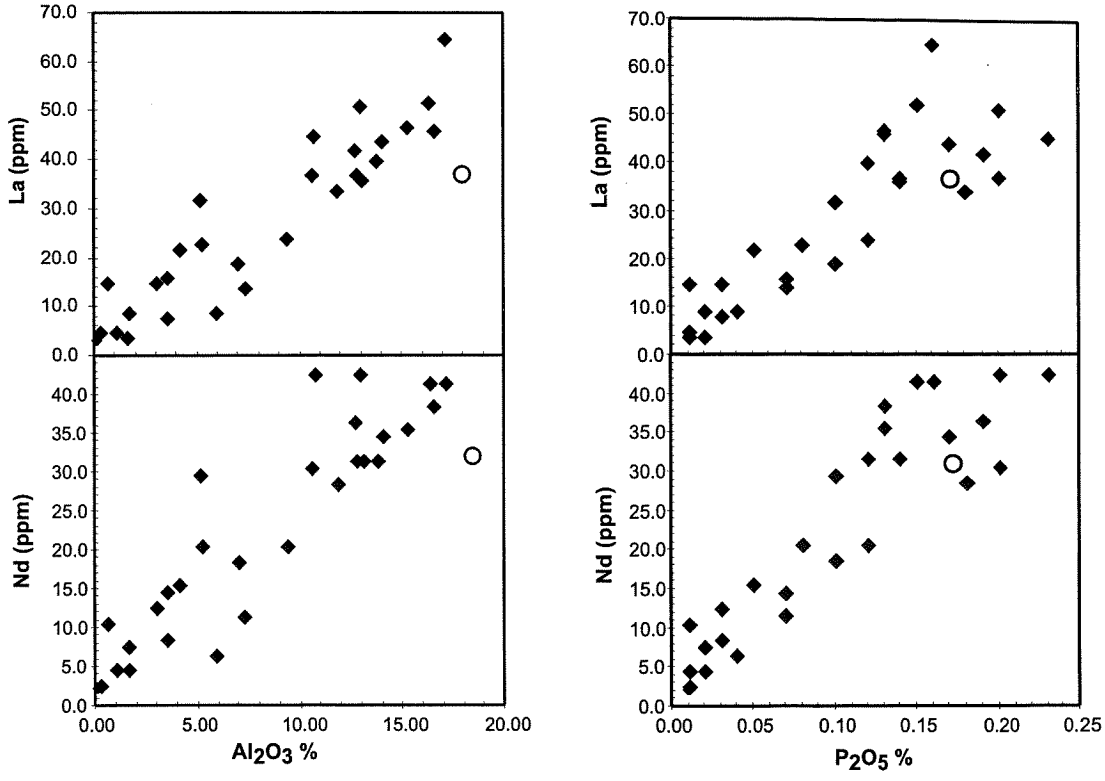

Fig. 4. REE-oxide variation diagrams for Officer Basin sedimentary rocks. Open circle = PAAS (Post-Archean Australian Shale, Taylor and McLennan, 1985).

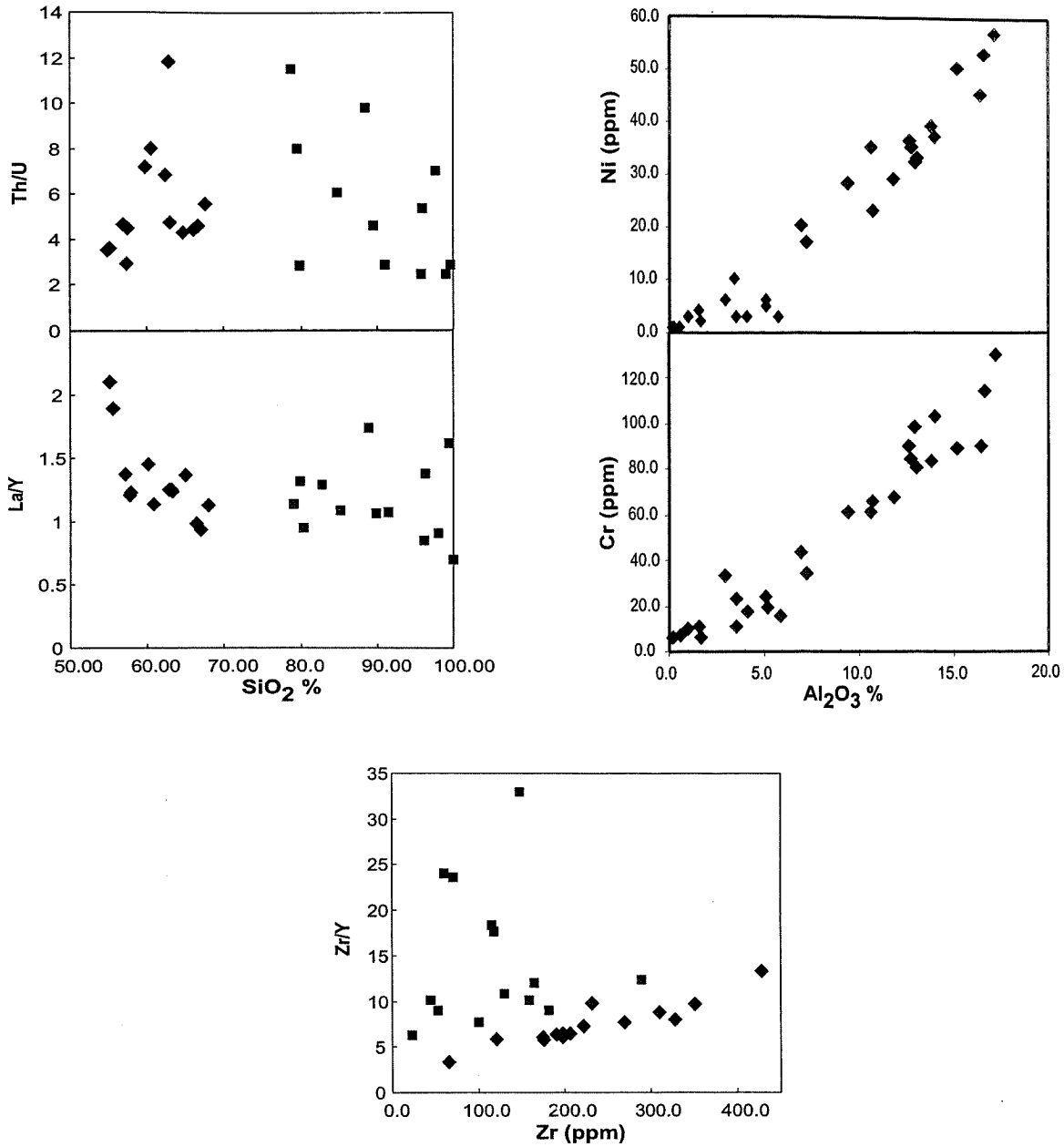

Fig. 5. Trace ratios vs oxide and compatible element vs oxide variation diagrams, (squares=sandstones, diamonds= mudstones/siltstones).

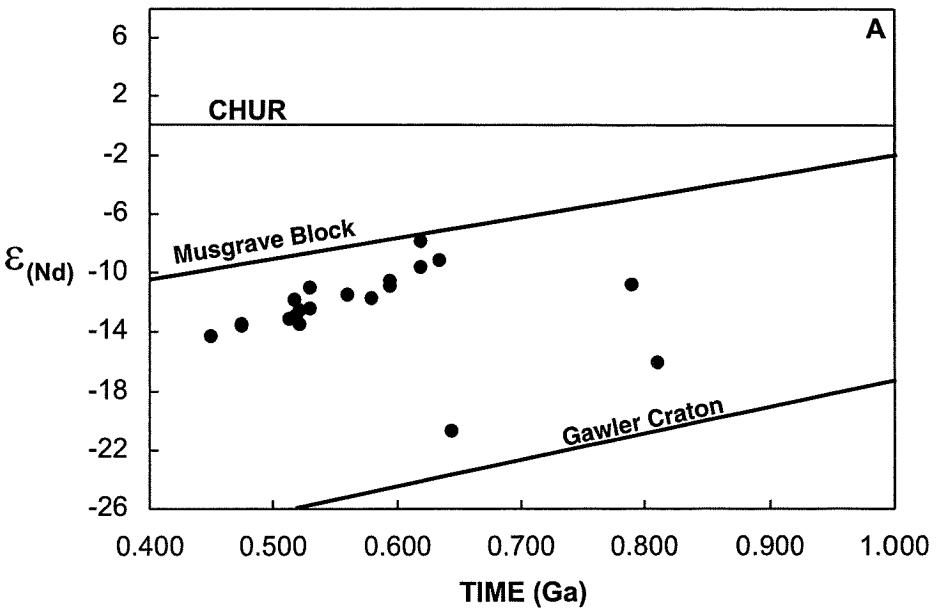

Fig. 6a. εNd versus time plots for Officer Basin samples. Average basement data for the Musgrave Block and Gawler Craton is plotted (Zhao et al., 1992; Turner et al., 1993; Creaser, 1995; Schaefer, 1998; Neumann, 2001). CHUR = bulk earth.

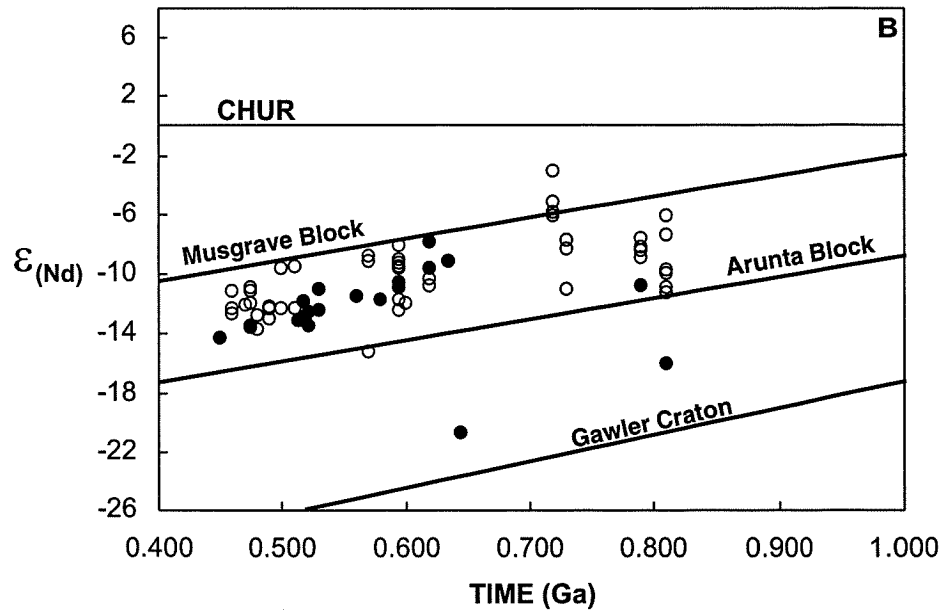

Fig. 6b. εNd versus time plots for Officer Basin samples and Amadeus Basin samples. Filled circles represent data from this study, and open circles are data from the Amadeus Basin north of the Musgrave Block (Zhao et al., 1992; Barovich and Foden, 2000; and unpublished data). Basement data for the Arunta Block, Musgrave Block and Gawler Craton as in Figure 6a). CHUR = bulk earth.

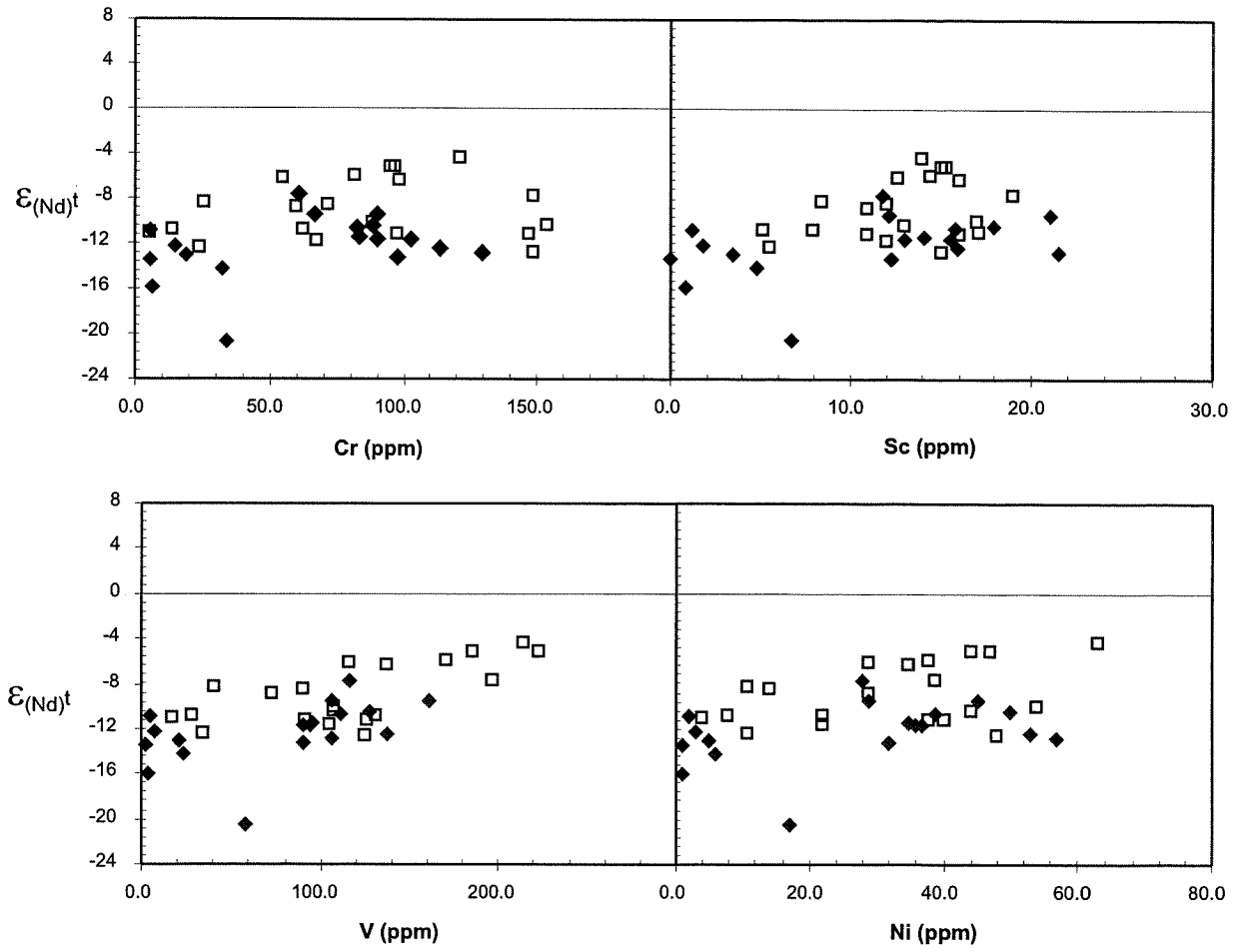

Fig. 7. Initial εNd versus mafic trace element indicators for Officer Basin, Amadeus Basin , and Adelaide Geosyncline sedimentary rocks. Filled diamonds represent data from this study, open squares represent data from Barovich and Foden (2000) and Turner et al. (1993). The rough positive trend of less negative εNd values and elevated Cr, Ni, Sc, and V for samples from the current study is interpreted as contribution from the Musgrave Block containing mafic material.

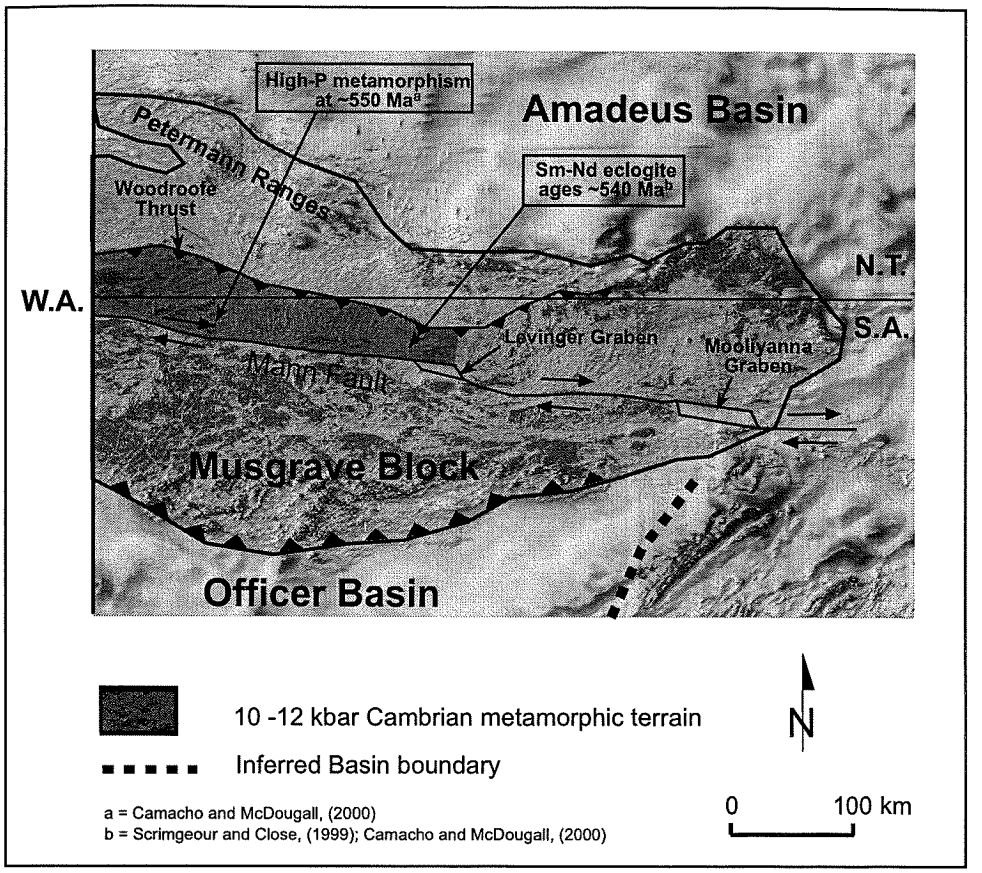

Fig. 8a. Grey scale TMI image of the Musgrave Block and associated structures. The Mann Fault may have acted as a extremely efficient sediment transport system for much of history of the Petermann Orogeny. North of the Mann Fault is a region of High *P* Cambrian metamorphism (Scrimgeour and Close, 1999; Camacho and McDougall, 2000).

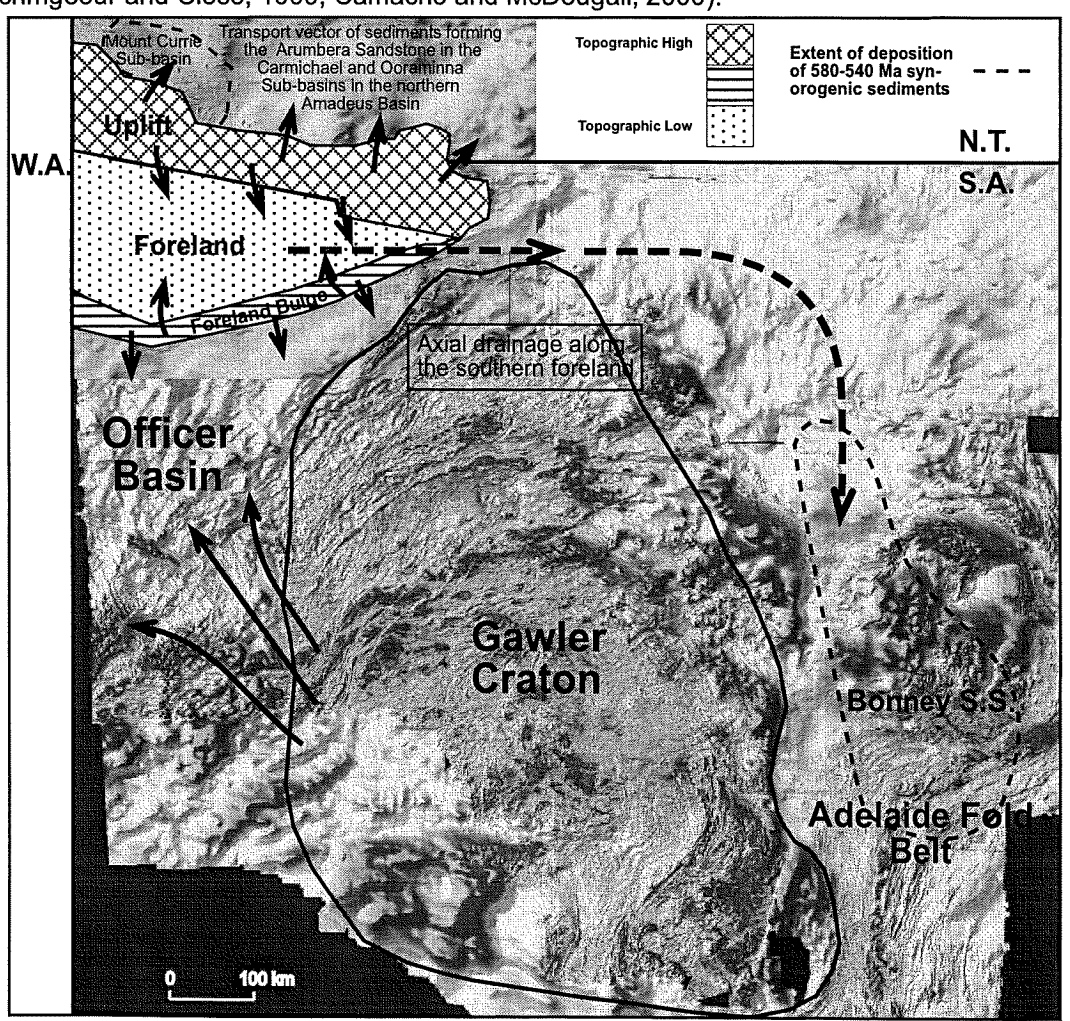

Fig. 8b. Gray scale TMI image showing possible differential uplift of the Musgrave Block. Possible sediment transport directions include eastwards into the Adelaide Fold Belt and northwards into the Amadeus Basin. (TMI image supplied by PIRSA pers comm Michael Schwarz)

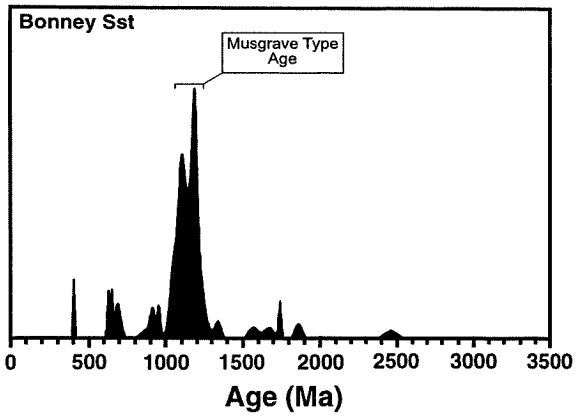

Fig. 9. Detrital zircon histogram of the 540 Ma Bonney Sandstone. The large population around 1100-1200 Ma are zircons typical of the Musgrave Block (Ireland et al., 1998).

Appendix 1

Sm-Nd data used for source characterisation

Source	$^{143}Nd/^{144}Nd$	$^{147}Sm/^{144}Nd$	Data Points	Author
Musgrave Block				
	0.511896	0.1181	20	Zhao et al., 1992
Average composition	0.511896	0.1181	20	
Gawler Craton				
	0.511422	0.1110	8	Turner et al., 1993
	0.511389	0.1067	8	Creaser, 1995
	0.511267	0.1060	10	Neumann, 2001
	0.511336	0.1187	14	Schaefer, 1998
Average composition	0.5113535	0.1106	40	